



ELSEVIER

Contents lists available at SciVerse ScienceDirect

## Information Sciences

journal homepage: [www.elsevier.com/locate/ins](http://www.elsevier.com/locate/ins)

# Improving feature space based image segmentation via density modification

Debashis Sen\*, Sankar K. Pal

Center for Soft Computing Research, Indian Statistical Institute, 203 B.T. Road, Kolkata, West Bengal 700 108, India

## ARTICLE INFO

### Article history:

Received 9 June 2009

Received in revised form 23 December 2011

Accepted 27 December 2011

Available online 4 January 2012

### Keywords:

Density modification

Fuzzy sets

Beam theory

Feature space analysis

Image segmentation

## ABSTRACT

Feature space based approaches have been popularly used to perform low-level image analysis. In this paper, a density modification framework that enhances density map based discriminability of feature values in a feature space is proposed in order to aid feature space based segmentation in images. The framework embeds a position-dependent property associated with each sample in the feature space of an image into the corresponding density map and hence modifies it. The property association and embedding operations in the framework is implemented using a fuzzy set theory based system devised with cues from beam theory of solid mechanics and the appropriateness of this approach is established. Qualitative and quantitative experimental results of segmentation in images are given to demonstrate the effectiveness of the proposed density modification framework and the usefulness of feature space based segmentation via density modification.

© 2012 Elsevier Inc. All rights reserved.

## 1. Introduction

Image segmentation is a critical component of low-level image analysis. Image segmentation is a process of dividing an image into different regions such that each region is uniform in a certain sense and the union of any two regions is not uniform.

Feature space analysis based approaches have been popularly used to perform image segmentation. Initial works resulting in such segmentation techniques were based on finding thresholds in gray-level (single feature) histograms of images [12,30,33,43] and they are still widely used due to their simplicity. Segmentation based on values of multiple features at various pixels in an image are performed by first obtaining the thresholds in one dimensional histograms corresponding to the different features and then by employing the thresholds in the underlying multidimensional feature space [20]. Such a multiple feature based image segmentation method is a monothetic approach, where each feature is separately considered for analysis. Clustering techniques, which are polythetic (simultaneous consideration of multiple features) in nature, are also used in multidimensional feature space to carry out image segmentation. A broad review of clustering based image segmentation approaches is given in [11].

Many thresholding, clustering and other decision making systems used for feature space based segmentation consider judicious but speculative formulations of the underlying problem [35]. For example, many histogram thresholding techniques are based on prior assumptions such as the histogram fits a particular model very well or valleys in the histogram represent class boundaries. Partitional clustering techniques such as c-means and its variations [6,18,22] make assumptions about prototypes and shapes of the clusters to be formed, mode seeking algorithms [1,3,11] assume local modes (maxima) in the density of the samples in the feature space as cluster prototypes and mixture resolving algorithms [6,11] assume that the

\* Corresponding author.

E-mail addresses: [dsen\\_t@isical.ac.in](mailto:dsen_t@isical.ac.in) (D. Sen), [sankar@isical.ac.in](mailto:sankar@isical.ac.in) (S.K. Pal).

density of the samples in the feature space appropriately fits a particular model. Hierarchical clustering algorithms [6,11] assume a specific function to measure the similarity between clusters in the feature space. Assumptions such as the aforesaid ones corresponding to various decision making algorithms may or may not be appropriate for the feature space based low-level image analysis task at hand as they may or may not be in harmony with the representation of various contents (regions) of an image in a feature space. For example, it is very difficult to ascertain that clusters formed in an image feature space using the c-means algorithm, where cluster means are considered as cluster prototypes, would correspond to the natural regions in the underlying image.

Let us now consider the perspective that many systems that perform segmentation through feature space analysis actually categorize the feature values in an image feature space based on the density map of samples in the feature space. Therefore, although it is difficult to ascertain the appropriateness of a system for a feature space based segmentation task, one way of improving its performance could be by using some additional useful information such that density map based discriminability of feature values in the underlying feature space is enhanced. In this paper, we suggest that in order to enhance density map based discriminability of feature values in an image feature space, additional useful information could be suitably embedded into the density map of samples in the feature space resulting in its modification. Segmentation could then be carried out considering the feature space with the modified density map. Note that, by density map, we refer to the density of samples at various positions (values of features) in a feature space and density map based discriminability of feature values essentially means the discriminability of feature values based on the distribution of samples in the corresponding feature space.

A few other density modification techniques designed to aid segmentation are reported in [9,43]. In [43], histogram modification is considered in order to aid valley seeking based threshold determination in gray-level feature spaces for image segmentation. A histogram transformation technique is proposed in [9] to aid the application of Gaussian mixture resolving algorithm in gray-level feature spaces for bi-level segmentation.

Note that, the aforesaid density modification approaches do not belong to the class of techniques referred to as image pre-processing (enhancement, smoothing, noise reduction, redundant information removal) [8,26,40], which is widely used for favorably transforming an image before segmentation. The aforesaid density modification approaches do not transform the image in order to aid image segmentation. Hence, they are very much a part of the segmentation process itself and they are not image pre-processing algorithms.

Methods for improving performance of segmentation systems by other means have also been presented in literature. In [31], an adaptive approach has been presented to improve the effectiveness of the thresholding technique of [30]. In [2,21], edge strengths at image pixels have been used to aid threshold determination for segmentation. In [25], an approach to ensemble different thresholding algorithms has been considered to increase the efficacy of threshold determination. Use of kernel functions [36] to make clustering more effective in the presence of nonlinearly separable classes has been popularly used [5,18,47] for image segmentation. Clustering has been improved in [41,45] by considering robustness towards noise and outliers. In [14], performance of a class of clustering methods is improved by achieving certain relaxation in an inherent optimization approach and simplification of mixture models is considered in [46] to make clustering efficient in practical applications. In [15], a new measure of cluster quality is considered to improve clustering performance in the presence of arbitrarily shaped classes. In [27], the concept of shadowed sets is used to improve the performance of c-means clustering algorithm for segmentation by efficiently handling overlapping among segments while modeling uncertainty among the boundaries. Performance of image segmentation using artificial immune system based clustering is improved in [44] by considering the fusion of complementary features representing image texture. Performance of image segmentation by rough set theoretic thresholding is improved in [23] by considering adaptation to spatial data relationships. In [19], segmentation based on fuzzy clustering is improved by creating a provision to define a prior distribution and finding the segments using fuzzy minimax approach. In [17], region-based image segmentation has been considerably enhanced by designing an effective approach to deal with intensity inhomogeneities. A Bayesian network model based interactive segmentation technique is presented in [48], where interventions are actively sought from human. This is an improvement over standard interactive segmentation techniques that passively depend on human to provide the exact intervention.

In this paper, we propose a density modification framework, which enhances density map based discriminability of feature values in a feature space, to aid feature space based segmentation of images. In the proposed framework, first, fuzzy set theory is used to associate a position (feature value) – dependent property with each sample in a feature space of an image and then this property is embedded into the corresponding density map resulting in its modification. We propose the use of beam theory from the field of solid mechanics to carry out the property association and embedding processes in the framework. We also establish that the use of beam theory based property association and embedding processes indeed enhances density map based discriminability of feature values in the underlying feature space. Segmentation is performed considering feature spaces with modified density map obtained using the proposed density modification framework. The effectiveness of the proposed density modification framework is demonstrated by qualitatively and quantitatively comparing the segmentation performances achieved with and without the use of the proposed framework. In addition, the novel approach of feature space based segmentation via density modification is compared to two popular and state-of-the-art segmentation approaches, both qualitatively and quantitatively.

The organization of the paper is as follows. In Section 2, the novel framework for density modification in a feature space of an image is presented. The processes of beam theory based density modification in one dimensional and multidimensional feature spaces are presented in Sections 3 and 4, respectively, along with their justifications. Experimental results showing

the effectiveness of the proposed density modification framework and the usefulness of feature space based segmentation via density modification through various kinds of comparisons are presented in Section 5. Section 6 concludes the paper.

## 2. A framework for density modification in a feature space of an image

In this section, we propose a framework to modify the density map of the samples in a feature space corresponding to an image in order to aid image segmentation based on feature space analysis by enhancing density map based discriminability of feature values in the feature space. The proposed framework incorporates useful information for enhancing the aforesaid discriminability leading to the modification.

Let every pixel in an image be associated with  $n$  real values ( $\in \mathbb{R}$ ) representing  $n$  different features. These values at a pixel are obtained by considering a local neighborhood around it. Let us consider that segmentation is to be performed based on the values of the  $n$  different features at each pixel in the image. In order to carry out the aforesaid tasks, a discrete  $n$ -dimensional space with real coordinates ( $\mathbb{R}^n$ ), where each dimension corresponds to a feature, is considered. Let us denote this  $n$ -dimensional space by  $S$  and refer to it as an  $n$ -dimensional feature space of an image. The bounds along a dimension in the  $n$ -dimensional feature space ( $S$ ) is given by the minimum and maximum values that the corresponding feature can take. Each pixel in the image is mapped onto  $S$  using the corresponding  $n$  values representing the  $n$  different features and hence the feature space is populated. This populated feature space, with a sample in it representing a pixel in the image, is referred to as an  $n$ -dimensional histogram, say  $H$ , of the image.

The aforesaid process of mapping image pixels to a feature space is referred to as the histogram method of estimating density of samples in the feature space [39]. Although there are inherent approximations associated with the histogram method of density estimation [39], it is a widely used class of density estimates. We shall denote the density map of the samples in  $S$  using  $f$  and consider it as the  $n$ -dimensional histogram  $H$ , without loss of generality. Note that, one may also obtain  $f$  by considering density estimation techniques [39] more complex and sophisticated than the histogram method. Segmentation, which is based on the values of different features at each pixel in an image, is usually carried out considering the density map  $f$ . We suggest here that one may modify the density map in a favorable manner before carrying out such tasks.

Let us now consider the discrete feature space  $S$  as a universe of positions and let  $I$  be an element (a position) in it, that is,  $I \in S$ . By positions in a feature space, we refer to the various values of features in the feature space. Note that,  $I \equiv (i_1, i_2, \dots, i_n)$ , where  $i_k (\in \mathbb{R})$  is the value in (of) the  $k$ th dimension (feature) and the density of the samples at  $I$  is given by  $f(I)$ . We suggest that the samples at every  $I$  (in a populated feature space) be associated with a suitable property, which is dependent on (a function of)  $I$  and hence we refer it to as a position (feature value) – dependent property, say,  $\mu(I)$ . This property, which provides useful information, then be suitably embedded into the density map of the samples in  $S$  resulting in its modification. If appropriate property association and embedding processes are considered, the modification would enhance density map based discriminability of feature values in the feature space and hence it would aid feature space based segmentation. The aforesaid processes of property association and embedding forms a framework for density modification in a feature space of an image. Fig. 1 gives a pictorial representation of this proposed framework.

In the property association block (see Fig. 1) of the proposed framework, a sample in an  $n$ -dimensional feature space ( $S$ ) of an image is associated with a property that depends on its position, which represents the values of the  $n$  features corresponding to the sample. For an example, consider the YUV space [42] of a color image as the feature space. A sample (a pixel in the color image) in the YUV space can be associated with a property ‘brightness’ that depends on the value of the Y component at its position. A sample with a larger Y value is considered ‘more bright’ than another with a smaller Y value. Properties such as the aforesaid ‘brightness’ can be readily represented using fuzzy sets [13]. A fuzzy set can be defined in a feature space such that the corresponding membership function relates the underlying property to the positions in the feature space [13,28,32].

In the property association block, a fuzzy set  $F$  in  $S$  is considered as follows:

$$F = \{(I, \mu(I)) | I \in S\}, \quad 0 \leq \mu(I) \leq 1 \quad (1)$$

where  $\mu$  is the membership function and  $\mu(I)$  gives the extent to which the position  $I$  holds the property represented by the fuzzy set  $F$  [13]. Therefore, the samples at every  $I \in S$  are associated with a property and this association is given by the value of the membership function  $\mu$  at  $I$ . Hence, the property at every  $I \in S$  is represented by  $\mu(I)$ .

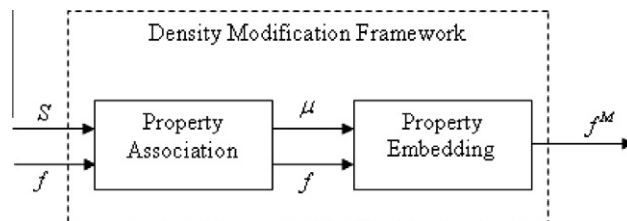


Fig. 1. The proposed density modification framework for feature space based segmentation.

In an  $n$ -dimensional feature space ( $S$ ) of an image, the property to be associated with the various positions can be considered to depend on the values of all the  $n$  different features. When such a property ( $\mu$ ) is considered in the property association block (see Fig. 1) of the proposed framework, the property can be assumed to be a combination of  $n$  properties, say  $\mu_k$ , with  $k = 1, 2, \dots, n$ , where  $\mu_k$  denotes a property that depends (is a function of) only on the value of the feature (at the various positions) that changes along the  $k$ th dimension in  $S$ .

In the property embedding block (see Fig. 1) of the proposed framework, the density  $f$  of the samples in  $S$  is modified using the associated property  $\mu$  as follows:

$$f^M = \Psi(\mu, f) \quad (2)$$

where  $f^M$  is the modified density map of the samples in  $S$ . The symbol  $\Psi$  represents the embedding process, where the underlying property is suitably embedded into the density map. For example, when  $\mu$  stands for the aforementioned property 'brightness', it may be embedded in such a way that distinguishing brighter image areas from the darker ones using YUV feature space becomes easier.

Now, segmentation based on the values of different features at each pixel in an image can be carried out considering the modified density map  $f^M$  of the samples in  $S$  instead of  $f$ . However, it is extremely important to ascertain the appropriateness of the property  $\mu$  and the suitability of the embedding process  $\Psi$ , so that the above proposed density modification framework benefits segmentation.

In the following sections, we shall show that beam theory [34] from the field of solid mechanics can be used to define  $\mu$  and  $\Psi$ , automatically and appropriately. Note that, the use of beam theory does not undermine the generality of the proposed framework, where any suitable  $\mu$  and  $\Psi$  can be used.

### 3. Density modification in one dimensional feature space: cues from beam theory

Consider a one dimensional feature space, say  $S_1$ , of an image and let the positions in  $S_1$  be represented by  $i_1$ . Let us consider that the density map, say  $f_1$ , of the samples in  $S_1$  is the corresponding one dimensional histogram of the image. We first normalize  $f_1$  as follows:

$$\bar{f}_1(i_1) = \frac{f_1(i_1)}{\sum_{z \in S_1} f_1(z)}, \quad i_1 \in S_1 \quad (3)$$

We then treat  $\bar{f}_1$  as the probability density function (PDF) of a random variable, which is considered to have generated the values of the underlying feature at the various pixels in the image. This PDF shall now be subjected to a beam theory based algorithm in order to calculate 'chance of sustainability' (see Section 3.2) at each  $i_1 \in S_1$ .

#### 3.1. Beam theory

As given in [34], "A member of a structure which is acted upon by forces perpendicular to its axis is called a beam. A beam which rests freely on two supports (pivots) is called a simply supported beam". Let us consider that a simply supported beam is being acted upon by a force or load  $P$  perpendicular to its axis. Under the assumption that the length of the beam is significantly larger than its width and depth, the displacement  $W$  of the beam in the direction of the force is governed by the Euler–Bernoulli beam equation [34], which is expressed as

$$\frac{d^2}{dx^2} \left( E(x) \times I(x) \times \frac{d^2 W(x)}{dx^2} \right) = P(x) \quad (4)$$

where  $E$  is the Young's modulus of the beam,  $I$  is the moment of inertia of the beam's cross-section and  $x$  is a variable that represents the position on the beam. The force  $P$  acting upon the beam generates a bending moment  $B$  [34], which is related to  $P$  as follows:

$$\frac{d^2 B(x)}{dx^2} = -P(x) \quad (5)$$

Therefore, using (5) in (4) we get

$$\rho(x) \approx -\frac{d^2 W(x)}{dx^2} = \frac{B(x)}{E(x) \times I(x)} \quad (6)$$

where  $\rho$  is referred to as the curvature of the beam [34]. In this paper, we shall consider the fact that the larger the curvature at a position  $x$  on the beam, the smaller the chance that the position sustains the force or load on it. We define a quantity called the 'chance of sustainability' at a position as the relative probability value, which represents the chance that the position sustains (against possible breakage) the force or load compared to the other positions. Note that, the sum of all the relative probability values, which represent 'chance of sustainability' at all the positions, is unity, as the probability that any one of the positions sustains is unity.

3.2. ‘Chance of sustainability’ calculation for a given density map in a one dimensional feature space

Here, we relate the density map in a one dimensional feature space to a force acting on a simply supported beam, the corresponding bending moment generated and the moment of inertia opposing the bending. After defining these relations, we present here the calculation of ‘chance of sustainability’ corresponding to the density map under consideration.

3.2.1. The Setup

Consider a simply supported beam of uniform (along the length) depth (height) and width with the pivots, say  $\alpha$  and  $\beta$ , at the two ends. Let the two ends refer to the two positions in the feature space  $S_1$  that correspond to the smallest and largest values of the underlying feature in the image under consideration. Let us consider that a uniform (along the length) force, say due to gravity, is always acting upon the uniform beam (the simply supported beam of uniform depth and width). We then consider that the uniform beam is loaded with a solid whose shape is given by the PDF  $\bar{f}_1$ . Let us assume that the entire uniform beam and the entire solid are made out of the same material. In this setup, the loaded solid augments with the uniform beam to act as a composite beam, and hence both the acting force and the opposing inertia depends on  $\bar{f}_1$ . We assume that the length of the composite beam is significantly larger than its width and depth so that Euler–Bernoulli beam equation (see (4)) is applicable. Fig. 2 gives the pictorial representation of the above explained setup.

From the above setup, let us now put down the relations between the quantities  $x$ ,  $P$  and  $\iota$  given in Section 3.1 and the density map  $f_1$  of the feature space  $S_1$ . We have  $x \equiv i_1$  and  $P(x) \equiv P(i_1) = \bar{f}_1(i_1) + \gamma_p$ , where  $i_1 \in S_1$  and  $i_1$  lies in the interval  $[e_a, e_b]$  with  $e_a$  and  $e_b$  denoting the two positions representing the two ends of the simply supported beam, that is, the smallest and largest values of the underlying feature in the image under consideration. The constant  $\gamma_p$  is due to the uniform force considered in the setup. We take the value of  $\gamma_p$  as  $(\sum_{i_1 \in S_1} f_1(i_1))^{-1}$ , which represents one unit (force) with respect to  $\bar{f}_1(i_1)$ . We also have  $\iota(x) \equiv \iota(i_1)$  with  $i_1 \in [e_a, e_b]$ , where  $\iota(i_1)$  is calculated (see Section 3.2.2) based on the quantity  $\bar{f}_1(i_1) + \gamma_p$ . The constant  $\gamma_i$  is due to the uniform beam and we consider this constant to be the smallest possible value given as  $(\sum_{i_1 \in S_1} f_1(i_1))^{-1}$ , that is, one unit (height) with respect to  $\bar{f}_1(i_1)$ .

3.2.2. The algorithm to calculate ‘chance of sustainability’

Once  $\bar{f}_1(i_1)$  is obtained from  $f_1(i_1)$  using (3), we calculate the bending moment  $B(i_1)$  due to the force  $P(i_1)$  at a position  $i_1 \in [e_a, e_b]$  (refer Fig. 2) as follows [34]:

$$B(i_1) = (R_x \times l) - (CP(i_1) \times (l - CG(i_1))), \text{ where } l = i_1 - e_a \tag{7}$$

In the above,  $CP(i_1)$  stands for the total (cumulative) force between the positions  $e_a$  and  $i_1$ , and it is given as

$$CP(i_1) = \sum_{z=e_a}^{i_1} P(z) = \sum_{z=e_a}^{i_1} (\bar{f}_1(z) + \gamma_p) \tag{8}$$

The symbol  $CG(i_1)$  stands for the center of gravity between the positions  $e_a$  and  $i_1$ , and it is given as

$$CG(i_1) = \frac{1}{CP(i_1)} \sum_{z=e_a}^{i_1} (z - e_a)P(z) \tag{9}$$

In (7),  $R_x$  is the reactive force at the pivot  $\alpha$  and it is calculated as

$$R_x = CP(e_b) \times \left[ \frac{L - CG(e_b)}{L} \right], \text{ where } L = e_b - e_a \tag{10}$$

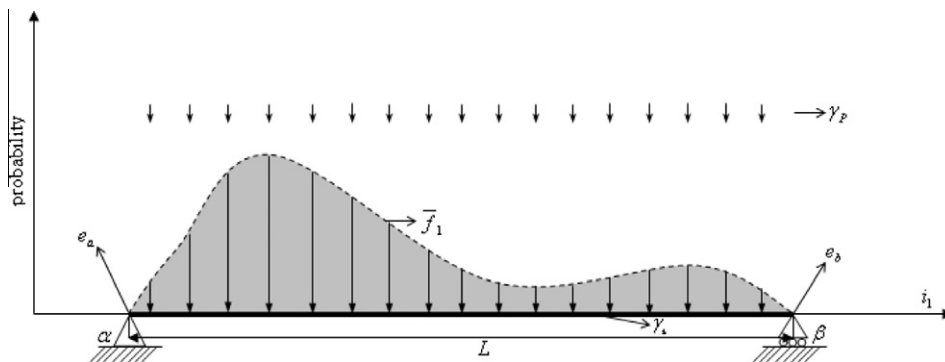


Fig. 2. The setup for ‘chance of sustainability’ calculation for a given density map in a one dimensional feature space.

As the entire composite beam is made out of the same material,  $E$  would have a fixed value along the length of the composite beam and without loss of generality we consider that value to be unity. We may then use (6) to calculate the curvature due to the bending moment  $B(i_1)$  at a position  $i_1 \in [e_a, e_b]$  as follows:

$$\rho(i_1) = \frac{B(i_1)}{I(i_1)} \quad (11)$$

where  $I(i_1)$  is the moment of inertia (opposing the bending) at  $i_1$ , which is calculated as

$$I(i_1) = \sum_{k=0}^{\bar{f}_1(i_1)+\gamma_i} (k - c(i_1))^2 \quad (12)$$

where  $c(i_1)$  denotes the centroid of the composite beam at position  $i_1$  and it is given by  $0.5 \times (\bar{f}_1(i_1) + \gamma_i)$ .

However, it is observed that a PDF  $\bar{f}_1$  may correspond to solids which when considered in the setup would result in curvature ( $\rho$ ) values that are very large at a few positions, making the values at other positions insignificant. We suggest that such situations are unfavorable for density modification in a feature space, as many originally populated positions in the space would be ignored during analysis based on the modified density. In order to circumvent such situations, we consider the following measure instead of  $\rho$  at a position  $i_1 \in [e_a, e_b]$ :

$$\hat{\rho}(i_1) = \frac{B(i_1)}{I(i_1) + \max_{z \in [e_a, e_b]} I(z)} \quad (13)$$

and then normalize  $\hat{\rho}$  as follows:

$$\bar{\hat{\rho}}(i_1) = \frac{\hat{\rho}(i_1)}{\sum_{z \in [e_a, e_b]} \hat{\rho}(z)}, \quad i_1 \in [e_a, e_b] \quad (14)$$

Once the value of  $\bar{\hat{\rho}}(i_1)$  for all  $i_1 \in [e_a, e_b]$  has been obtained, we perform the following operation:

$$\theta(i_1) = \max_{z \in [e_a, e_b]} \bar{\hat{\rho}}(z) - \bar{\hat{\rho}}(i_1) + \frac{\max_{z \in [e_a, e_b]} \bar{\hat{\rho}}(z)}{C} \quad (15)$$

where  $C \in \mathbb{Z}^+$ , where  $\mathbb{Z}^+$  stands for set of positive integers. We then normalize  $\theta$  as follows:

$$\bar{\theta}(i_1) = \frac{\theta(i_1)}{\sum_{z \in [e_a, e_b]} \theta(z)}, \quad i_1 \in [e_a, e_b] \quad (16)$$

As mentioned in Section 3.1, we consider that the larger the curvature  $\rho$  at a position, the smaller the ‘chance of sustainability’ at that position. From (15) and (16), we see that the larger the value of  $\hat{\rho}$  at a position, the smaller the value of  $\bar{\theta}$  at that position. Now, as  $I(i_1) + \max_{z \in [e_a, e_b]} I(z)$  is linearly and positively correlated to  $I(i_1)$ , it is evident from (13) that  $\hat{\rho}$  is positively correlated to  $\rho$ . Therefore, we see that the larger the value of the curvature  $\rho$  at a position, the smaller the value of  $\bar{\theta}$  at that position. We consider the measure  $\bar{\theta}$  at a position as the ‘chance of sustainability’ at that position. Note that, we consider the term  $\frac{\max_{z \in [e_a, e_b]} \bar{\hat{\rho}}(z)}{C}$  in (15) in order to ensure that ‘chance of sustainability’ at a position is a nonzero quantity, as a zero ‘chance of sustainability’ would mean that the position has no resistance to the applied load which is intuitively unappealing.

### 3.3. Deduction of modified density map from ‘chance of sustainability’ values in a one dimensional feature space

We consider the distribution of ‘chance of sustainability’ ( $\bar{\theta}$  values) with respect to the various positions ( $i_1$  values) in the interval  $[e_a, e_b]$  of the one dimensional feature space  $S_1$  to get a PDF, say  $\bar{f}_1^M$ , as follows:

$$\bar{f}_1^M(i_1) = \begin{cases} \bar{\theta}(i_1) & i_1 \in [e_a, e_b] \\ 0 & i_1 \notin [e_a, e_b] \end{cases} \quad (17)$$

We say that a beam theory based modification process applied on the PDF  $\bar{f}_1$  has yielded the PDF  $\bar{f}_1^M$ . Now, a density map, say  $f_1^M$ , which corresponds to  $\bar{f}_1^M$  for all  $i_1 \in S_1$ , is obtained as follows:

$$f_1^M(i_1) = \text{round} \left( \bar{f}_1^M(i_1) \times \left( \frac{C}{\max_{z \in [e_a, e_b]} \bar{\hat{\rho}}(z)} \times \sum_{z \in [e_a, e_b]} \theta(z) \right) \right) \quad (18)$$

The density map  $f_1^M$  in the one dimensional feature space  $S_1$  can be considered as a modified density map obtained using the proposed density modification framework (see Section 2) on the density map  $f_1$  of the samples in  $S_1$ . With such a consideration, the bending moment  $B$  would be a quantity given by the underlying membership function multiplied by a constant and hence the expressions in (7)–(10), which give the determination of the bending moment, would represent the property association process in the framework. The expressions in (12)–(18), where the moment of inertia  $I$ , which is a function of  $f_1$ ,

is combined with bending moment  $B$ , would represent the property embedding process in the framework. However, we need to ascertain that the underlying membership function and the embedding process are appropriate in order to consider that the use of the modified density map  $f_1^M$  instead of  $f_1$  would benefit feature space based segmentation.

### 3.4. Appropriateness of the density modification process in the context of feature space based image segmentation

#### 3.4.1. Appropriateness of the membership function

Let  $\mu_1$  be the underlying membership function, which relates a property to the positions ( $i_1$ ) in  $S_1$ , corresponding to the density modification framework used to get  $f_1^M$  from  $f_1$ . As mentioned earlier, the bending moment  $B$  is related to  $\mu_1$  and the relation is as follows:

$$\mu_1(i_1) = \frac{B(i_1)}{\max_{z \in [e_a, e_b]} B(z)}, \quad i_1 \in [e_a, e_b] \quad (19)$$

In order to ascertain the appropriateness of  $\mu_1$ , let us consider its following attributes:

- A1. *Nonnegativity* – It is evident from (7) that  $B(i_1) \geq 0$  for all  $i_1 \in [e_a, e_b]$  and hence from (19) we get  $\mu_1(i_1) \geq 0$  for all  $i_1 \in [e_a, e_b]$ .
- A2. *Range* – From attribute A1 and the observation that  $\sup_z \mu_1(z) \equiv \max_{z \in [e_a, e_b]} \mu_1(z) = 1$  (see (19)), we get that  $0 \leq \mu_1(i_1) \leq 1$  for all  $i_1 \in [e_a, e_b]$ .
- A3. *Vanish Identically* – It is easily deducible from (7) that  $B(i_1) = 0$  only when  $i_1 = e_a$  or  $i_1 = e_b$  and hence from (19) we get  $\mu_1(i_1) = 0$  only when  $i_1 = e_a$  or  $i_1 = e_b$ .
- A4. *Concavity* – When the interval  $[e_a, e_b]$  is considered as an interval in the real line, it becomes evident from Section 3.1 that the bending moment  $B$  would have a second derivative  $B''$  in  $[e_a, e_b]$  and  $B''(x) \leq 0$  for all  $x \in [e_a, e_b]$  as  $P(x) \geq 0$  for all  $x \in [e_a, e_b]$ . This condition  $B''(x) \leq 0$  is a necessary and sufficient condition for  $B$  to be a concave function. Hence, from (19) we get that  $\mu_1$  is a concave function on the interval  $[e_a, e_b]$ .

From attribute A2 it is evident that  $\mu_1$  can indeed be considered as a membership function corresponding to a fuzzy set. From attributes A3 and A4, we say that the value of the membership function  $\mu_1$  at a position  $i_1$  represents a property ‘farness of the position from the nearest pivot’, where the nearest pivot corresponds to either the smallest or the largest value of the underlying feature in the image considered. Note that, the aforesaid terms ‘farness’ and ‘nearest’ are inherently defined in  $\mu_1$ . The feature value (position  $i_1$ ), where  $\mu_1(i_1)$  takes a value of unity, is the position that is equally far from both the smallest and largest values of the feature. A feature value smaller (larger) than that position is nearer to the smallest (largest) value of the feature compared to the largest (smallest) value of the feature.

The aforementioned property ( $\mu_1$ ) would be a very useful one for feature space based segmentation, as the groups of samples in an image feature space associated with the smallest and largest values of a feature are the most discriminable from each other with respect to that feature. Moreover, in feature space analysis of an image, the samples having the smallest and largest values of a feature should never be categorized together with respect to that feature. Therefore, additional (other than that given by the density map  $f_1$ ) useful information is provided by the property ‘farness from the nearest pivot’, that is, ‘farness from the nearest among the smallest and largest values of the underlying feature’ and hence the membership function  $\mu_1$  is appropriate.

Now, it is evident from (7) and (19),  $\mu_1$  is dependent on the density map  $f_1$ . However, one might like to have the property ‘farness from the nearest among the smallest and largest values of the underlying feature’ in the image considered such that it depends only on the position ( $i_1$ ) and not on the density map ( $f_1$ ). Note that, if the value of  $\gamma_p$  is considered such that  $\gamma_p \gg \max_{z \in [e_a, e_b]} \hat{f}_1(z)$ , the membership function approximately becomes independent of  $f_1$  and depends only on  $i_1$ .

Note that, in the above discussion we assume that the underlying one dimensional feature space (universe  $S_1$ ) is a totally ordered set, that is, the feature values (positions) in the feature space can be uniquely ordered in an increasing or a decreasing manner. One dimensional feature spaces corresponding to most image features such as those in [10], intensity and RGB color components are totally ordered sets and hence they are in accordance with the aforesaid assumption. An example of a one dimensional feature space of an image that is not a totally ordered set is the one corresponding to the hue feature (in a color image).

#### 3.4.2. Appropriateness of the embedding process

As mentioned earlier, the expressions in (12)–(18) represent the property embedding process. Among the expressions in (12)–(18), the basic theme of embedding the property  $\mu_1$  associated with every position  $i_1 \in S_1$  into the density map  $f_1$  is given by (13), where  $B$ , which is related to  $\mu_1$ , is combined with  $\iota$ , which is a function of  $f_1$ . The values of the  $\hat{\rho}$  measure, which is positively correlated to the curvature  $\rho$ , at each position in  $S_1$  are calculated in (13) and then some algebraic manipulations are carried out to get the corresponding ‘chance of sustainability’ values that essentially represent the modified density map. The use of ‘chance of sustainability’ to get the modified density map ensures that the larger the curvature  $\rho$  at a position in  $S_1$ , the smaller the density at that position.

In order to ascertain that the embedding process is appropriate, consider the following analysis. From the calculation of ‘chance of sustainability’ values in (12)–(16) and its relation to  $\mu_1$  and  $f_1$ , we infer that the embedding process modifies the density at a position such that:

1. The modified density is larger (smaller) at a position when the value of  $f_1$  at that position is larger (smaller), for a fixed value of  $\mu_1$  at that position.
2. The modified density is larger (smaller) at a position when the value of  $\mu_1$  at that position is smaller (larger), for a fixed value of  $f_1$  at that position.

From the first aforesaid aspect, we see that the order among  $f_1$  values at all positions would be maintained (larger remains larger and smaller remains smaller) when  $\mu_1$  takes a fixed value at all the positions. Hence, we may indeed say that in the density modification process,  $\mu_1$  gets embedded into  $f_1$  resulting in its modification.

From Section 3.4.1, we infer that a larger value of  $\mu_1$  at a position means that the position is not nearer to any of the two mutually most discriminable groups of samples in the underlying feature space, which are at the two positions representing the smallest and largest values of the feature considered. Now, in order to aid feature space based segmentation, the density modification process should enhance the density map based discriminability of feature values (positions) in the feature space. Therefore, the modified density at a position should be larger (smaller) when the value of  $\mu_1$  at that position is smaller (larger), so that, more samples are nearer to any of the two mutually most discriminable groups of samples.

From the second aforesaid aspect about the embedding process, we see that the modified density map obtained after the embedding process is such that more samples are nearer to any of the two mutually most discriminable groups of samples in the feature space compared to the density map before modification. Therefore, the embedding process indeed enhances the density map based discriminability of feature values in the feature space and hence the embedding process is appropriate.

Note that, from the relation between ‘chance of sustainability’ value and curvature value at a position (see Section 3.2.2), we find that the appropriate embedding process is such that the larger the curvature at a position in a feature space, the smaller the modified density at that position.

Let us consider now the example of gray-level feature based segmentation of the grayscale image given in Fig. 3a in order to see whether the embedment of the property  $\mu_1$  that provides useful information (as justified in Section 3.4.1) aids feature space based segmentation.

Fig. 3b shows the gray-level feature space populated with samples that correspond to the pixels in the image in Fig. 3a. As can be seen from the Fig. 3b, the density of the samples in the feature space is uniform with respect to the underlying gray levels. We deliberately consider such a case so that the effect of the embedment becomes clearly evident. Mode seeking algorithms such as the one in [3] and algorithms based on ambiguity minimization such as the one in [33] fail to segment the image, when they are applied to the gray-level feature space in Fig. 3b. Whereas, when the c-means algorithm and its variations or homogeneity based algorithms such as the one in [30] are applied, segmentation is achieved. These algorithms give the segmentation result shown in Fig. 3d.

Fig. 3c shows the modified density map obtained using the proposed beam theory based density modification scheme (see (18)) on the density map of the gray-level feature space shown in Fig. 3b. All the aforementioned algorithms successfully segment the image in Fig. 3a to get the result given in Fig. 3d, when they are applied to the gray-level feature space with the modified density shown in Fig. 3c. Various c-means type algorithms and homogeneity based techniques, which achieve segmentation in both the aforesaid cases, are found to be more powerful (in terms of discriminability) in performing the separation, when used on the gray-level feature space with the modified density.

The above observations suggest that density map based discriminability of the various feature values (positions) in a one dimensional image feature space is enhanced by performing the embedment of the property  $\mu_1$ . Hence, the embedment of the property  $\mu_1$  would aid (one dimensional) feature space based segmentation, like the example of image segmentation shown in Fig. 3.

The above analyses shows that beam theory from the field of solid mechanics can be used to define the  $\mu$  and  $\Psi$  (see Section 2), automatically and appropriately, when one dimensional feature space of an image is considered.

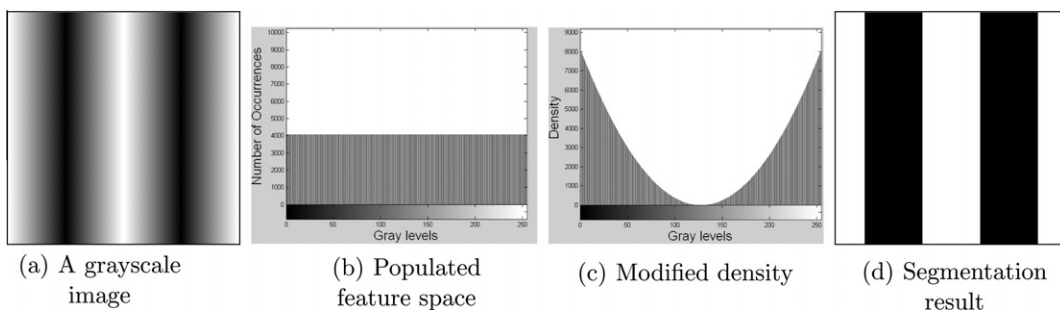


Fig. 3. Gray-level feature based segmentation in an image for judging appropriateness of the embedding process.

Note that, the number of samples corresponding to any feature value (position) in the range  $[e_a, e_b]$  is at least one and at most  $C + 1$  in the modified density map obtained in (18). It is also to be noted that the total number of samples in the modified density map might not be equal to that in the density map before modification. The expression in (18) could be designed in such way that the number of samples in the modified density map equals that in the density map before modification. However, in such a case the exact form of the PDF in (17) might not be reflected in the modified density map and hence we do not consider it. In other words, unlike the case of the density before modification, in the case of the modified density, samples in the feature space does not have one-to-one correspondence with image pixels. In order to perform segmentation, the outcome of a modified density based analysis performed on a one dimensional feature space of an image is mapped onto the pixels in the image with respect to the associated feature value. For example, in Fig. 3, the aforementioned algorithms applied on gray-level feature space with the modified density map divides the feature space into two parts, where the gray values in the range  $[1, 127]$  forms one part and the gray values in the range  $[128, 255]$  forms the other. The two corresponding regions in the image shown in Fig. 3a are obtained by separating all the pixels in the image having gray values in the range  $[1, 127]$  from those having gray values in the range  $[128, 255]$  (see Fig. 3d).

#### 4. Density modification in multidimensional feature space

As considered in Section 2, let  $S$  be an  $n$ -dimensional feature space of an image and let the positions in  $S$  be represented by  $I$ . Let us also consider that the density map  $f$  of the samples in  $S$  is the corresponding  $n$ -dimensional histogram. We first normalize  $f$  as follows:

$$\bar{f}(I) = \bar{f}(i_1, i_2, \dots, i_n) = \frac{f(I)}{\sum_{z \in S} f(z)}, I \in S \quad (20)$$

where  $i_k$  is the value in the  $k$ th dimension and each dimension in the space corresponds to a feature. We then treat  $\bar{f}$  as the multivariate PDF of random variables, which are considered to have generated the values of the underlying features at the various pixels in the image.

To carry out density modification in multidimensional feature space, we use the beam theory based process for density modification in one dimensional feature space introduced in the previous section. We do so by considering conditional PDFs giving the probabilities corresponding to one feature, when specific values of the other features are given. The conditional PDF giving the probabilities corresponding to a feature, which is represented by  $i_1$ , is expressed as

$$\bar{f}(i_1/i_2, i_3, \dots, i_n) = \frac{\bar{f}(i_1, i_2, \dots, i_n)}{\sum_{i_1} \bar{f}(i_1, i_2, \dots, i_n)} \quad (21)$$

Note that, the PDF  $\bar{f}(i_1/i_2, i_3, \dots, i_n)$ , for specific values of  $i_k$  with  $k = 2, 3, \dots, n$ , is a function of  $i_1$  alone and hence it is a one dimensional quantity. The beam theory based process proposed in Section 3.2.2 is applied on  $\bar{f}(i_1/i_2, i_3, \dots, i_n)$  to get the corresponding  $\bar{\rho}(i_1)$  values for all  $i_1 \in [e_a, e_b]$ , with the constants  $\gamma_p$  and  $\gamma_l$  equaling  $(\sum_{z \in S} f(z) \times \sum_{i_1} \bar{f}(i_1, i_2, \dots, i_n))^{-1}$ . Note that,  $e_a$  and  $e_b$  respectively corresponds to the smallest and largest value of the underlying feature at those pixels in the image where the other features have the considered specific values. The  $\bar{\rho}(i_1)$  values are then used to get a conditional PDF (a one dimensional quantity) as given below:

$$g_{i_1}(i_1/i_2, i_3, \dots, i_n) = \begin{cases} \bar{\rho}(i_1) & i_1 \in [e_a, e_b] \\ 0 & i_1 \notin [e_a, e_b] \end{cases} \quad (22)$$

and then using  $g_{i_1}(i_1/i_2, i_3, \dots, i_n)$ , we get:

$$g_{i_1}(i_1, i_2, \dots, i_n) = g_{i_1}(i_1/i_2, i_3, \dots, i_n) \times \sum_{i_1} \bar{f}(i_1, i_2, \dots, i_n) \quad (23)$$

where  $g_{i_1}(i_1, i_2, \dots, i_n)$ , for specific values of  $i_k$  with  $k = 2, 3, \dots, n$ , is a one dimensional quantity. When all such one dimensional quantities deducible from the conditional PDF in (21) are obtained by considering all possible values of  $i_k$  for all  $k = 2, 3, \dots, n$ , we get an  $n$ -dimensional quantity expressed as  $g_{i_1}(I)$  at a position  $I \in S$ . We also define a set  $\Omega_{i_1}$  in the  $n$ -dimensional feature space ( $S$ ) having all those positions ( $I$ ) as elements, where we find  $i_1 \notin [e_a, e_b]$  (see (22)) during the calculation of  $g_{i_1}$ .

Next, we obtain all  $g_{i_z}$  and  $\Omega_{i_z}$  with  $z = 1, 2, \dots, n$ , in a manner similar to the one described above. We then obtain a set, say  $\Omega$ , in  $S$  as follows

$$\Omega = \bigcap_{z=1}^n \Omega_{i_z} \quad (24)$$

It is evident from (22) and (23) that the value of  $g_{i_z}$  at a position  $I \in S$  is linearly and positively correlated to the corresponding  $\bar{\rho}(i_z)$ . As mentioned earlier in Section 3.2.2,  $\bar{\rho}(i_z)$  is positively correlated to the curvature  $\rho(i_z)$ . Hence,  $g_{i_z}(I)$  is positively correlated to the corresponding curvature  $\rho(i_z)$ .

After obtaining all  $g_{i_z}$  with  $z = 1, 2, \dots, n$ , we combine them as follows:

$$g(I) = \sqrt{g_{i_1}^2(I) + g_{i_2}^2(I) + \dots + g_{i_n}^2(I)}, \quad I \in S, \quad I \notin \Omega \quad (25)$$

where it is obvious that  $g(I)$  is positively correlated to the quadratic mean (root mean square) of the  $n$  curvatures (corresponding to the  $n$   $g_{i_z}$ s) associated with the position  $I$ . We then normalize  $g$  as follows

$$\bar{g}(I) = \frac{g(I)}{\sum_{y \in S, y \notin \Omega} g(y)}, \quad I \in S, \quad I \notin \Omega \quad (26)$$

The following operation is then carried out:

$$\Theta(I) = \max_{y \in S, y \notin \Omega} \bar{g}(y) - \bar{g}(I) + \frac{\max_{y \in S, y \notin \Omega} \bar{g}(y)}{C} \quad (27)$$

where  $C \in \mathbb{Z}_+$ , where  $\mathbb{Z}_+$  stands for set of positive integers. We then normalize  $\Theta$  as follows:

$$\bar{\Theta}(I) = \frac{\Theta(I)}{\sum_{y \in S, y \notin \Omega} \Theta(y)}, \quad I \in S, \quad I \notin \Omega \quad (28)$$

From (27) and (28), we see that the larger the value of  $g$  at a position, the smaller the value of  $\bar{\Theta}$  at that position. As  $g$  is positively correlated to the root mean square of the  $n$  curvatures, we consider the measure  $\bar{\Theta}$  at a position as the ‘chance of sustainability’ at that position. Note that, when  $n = 1$ ,  $\bar{\Theta}$  in (28) will equal  $\bar{\theta}$  in (16).

In the case of 2-dimensional feature space of an image, cues from classical plate theory [29] could be used to get the ‘chance of sustainability’ values. However, we consider the above explained approach of ‘chance of sustainability’ calculation even in the case of 2-dimensional feature space as it circumvents many complexities involved with the use of classical plate theory.

We then use the values of  $\bar{\Theta}$  at the various positions in  $S$  in order to get a PDF, say  $\bar{f}^M$ , as follows:

$$\bar{f}^M(I) = \begin{cases} \bar{\Theta}(I) & I \notin \Omega \\ 0 & I \in \Omega \end{cases} \quad (29)$$

We say that a beam theory based modification process applied on the PDF  $\bar{f}$  has yielded the PDF  $\bar{f}^M$ . Now, a density map, say  $f^M$ , which corresponds to  $\bar{f}^M$  for all  $I \in S$ , is obtained as follows:

$$f^M(I) = \text{round} \left( \bar{f}^M(I) \times \left( \frac{C}{\max_{y \in S, y \notin \Omega} \bar{g}(y)} \times \sum_{y \in S, y \notin \Omega} \Theta(y) \right) \right) \quad (30)$$

The density map  $f^M$  in the  $n$ -dimensional feature space  $S$  can be considered as a modified density map obtained using the proposed density modification framework (see Section 2) on the density map  $f$  of the samples in  $S$ . We now need to ascertain the appropriateness of the membership function  $\mu$  and the embedding process  $\Psi$  (see Section 2), which are inherent in the aforementioned density modification process, in order to consider that the use of the modified density map  $f^M$  instead of  $f$  would benefit feature space based segmentation.

#### 4.1. Appropriateness of the density modification process in the context of feature space based image segmentation

##### 4.1.1. Appropriateness of the membership function

From Section 3, we see that the quantity  $\bar{\rho}$  is associated with a membership function which represents a property that gives the farness of a position in the underlying one dimensional feature space from the nearest among the smallest and largest values of the feature in the image considered. From the explanation following (21) and (22), we see that the  $n$ -dimensional quantity  $g_{i_z}$ , for a particular value of  $z$ , is obtained based on different  $\bar{\rho}$  corresponding to different conditional PDFs that are functions of only the feature value that changes along the  $z$ th dimension in  $S$ .

Therefore, we infer that  $g_{i_z}$ , for a particular value of  $z$ , is inherently associated with a property (membership function), say  $\mu_z$ , which is dependent only on the value of the feature that changes along the  $z$ th dimension in  $S$ . This membership function represents an  $n$ -dimensional quantity which is formed by the aggregation of one dimensional quantities represented by the various membership functions associated with the different  $\bar{\rho}$  considered. The membership function  $\mu_z$  represents a property that gives the farness of a position in the underlying  $n$ -dimensional feature space  $S$  from the nearest among the corresponding smallest and largest values of the feature, whose value changes along the  $z$ th dimension in  $S$ , in the image considered.

Now, the quantity  $g$  obtained in (25) is based on all the  $g_{i_z}$  quantities, with  $z = 1, 2, \dots, n$ , and hence it is associated with  $n$  properties, with each of them giving the farness of a position in the underlying  $n$ -dimensional feature space  $S$  from the nearest among the corresponding smallest and largest values of one of the  $n$  features in the image considered. The membership function  $\mu$ , which represents the property considered in the density modification process, is inherent in  $g$  and it is given by a combination of the  $n$  properties, that is  $\mu_z$ , with  $z = 1, 2, \dots, n$ . Note that, from (25), it can be easily deduced that the aforesaid combination is such that  $\mu$  is positively correlated to a  $\mu_z$  for a particular value of  $z$ , considering  $\mu_z$  for other values of  $z$  as

fixed values. Therefore, it would be appropriate to say that  $\mu$  represents the property ‘farness of a position in an  $n$ -dimensional feature space  $S$  from all the nearest among the corresponding smallest and largest values of all the underlying features’ in the image considered.

The aforesaid property represented by  $\mu$  is an useful one for feature space based segmentation, as it represents the farness of every position (feature value) in an image feature space from the nearest among the mutually most discriminable groups (see Section 3.4.1) of samples in the feature space with respect to every feature considered. Therefore, additional (other than that given by the density map  $f$ ) useful information is provided by the property ‘farness from all the nearest among the corresponding smallest and largest values of all the underlying features’ and hence the membership function  $\mu$  is appropriate.

#### 4.1.2. Appropriateness of the embedding process

The expressions in (25)–(30) and the calculation of all the  $\bar{\rho}$  quantities (see (13) and (14)) corresponding to all  $g_i$  in (25) represent the property embedding process. Now, as mentioned earlier,  $g$  (see (25)) at a position is positively correlated to the root mean square of the  $n$  curvatures associated with that position. Note that, the algebraic manipulation carried out in this section to get the ‘chance of sustainability’ ( $\Theta$ ) values ( $\forall I \in S$ ) from  $g$ , which is positively correlated to the root mean square of the underlying  $n$  curvatures, are similar to that used in Section 3 to get the ‘chance of sustainability’ ( $\theta$ ) values ( $\forall i_1 \in S_1$ ) from  $\rho$ , which is positively correlated to the solitary underlying curvature. Therefore, similar to the case in Section 3, the use of ‘chance of sustainability’ to get the modified density  $f^M$  ensures that the larger the curvature at a position in the feature space, the smaller the density at that position, where the curvature at a position in the  $n$ -dimensional feature space is given by the root mean square of the  $n$  curvatures associated with that position.

It has been found in Section 3.4.2 that if the modified density obtained after the property embedding process is such that the larger the curvature at a position in a feature space, the smaller the density at that position, then the embedding process is appropriate. Therefore, the modified density map ( $f^M$ ) obtained in (30) corresponds to an appropriate embedding process and it would aid feature space based segmentation with an enhanced density map based discriminability of feature values in the feature space.

Note that, similar to the case in Section 3, in the modified density map obtained in (30), the number of samples corresponding to any feature value (position) within the set  $\Omega$  is at least one and at most  $C + 1$ . The total number of samples in the modified density map might not be equal to that in the density map before modification, and in order to perform segmentation, the outcome of a modified density based analysis performed on a feature space of an image is mapped onto the pixels in the image with respect to the associated feature values.

The above explanation and the explanation in Section 3 suggest that beam theory from the field of solid mechanics can be used to define the  $\mu$  and  $\Psi$  (see Section 2), automatically and appropriately.

## 5. Experimental results

In this section, the effectiveness of the proposed density modification techniques based on cues from beam theory is demonstrated by qualitatively and quantitatively comparing feature space based segmentation performances achieved with and without the use of the proposed framework. In addition, the novel approach of feature space based segmentation via density modification is qualitatively and quantitatively compared to two popular and state-of-the-art segmentation approaches. We consider  $C = 50$  throughout this section.

Segmentation of grayscale and color images based on feature space analysis is considered in order to carry out the aforesaid comparisons. Note that, we shall use the term ‘modified density’ in order to refer to a density map obtained after applying the proposed density modification scheme on the original density map of the samples that correspond to the pixels in the underlying image.

### 5.1. Comparison of performances achieved with and without the use of the proposed density modification framework

Here, we demonstrate the effectiveness of the proposed density modification framework by qualitatively and quantitatively comparing feature space based segmentation performances achieved with and without the use of the said framework.

#### 5.1.1. Qualitative analysis

**5.1.1.1. Segmentation in grayscale images based on gray-level feature.** Consider the segmentation of grayscale images shown in Fig. 4. The various segmentation results shown in the figure are achieved by obtaining thresholds in one dimensional gray-level feature spaces with original ( $f$ ) or modified ( $f^M$ ) density maps corresponding to the grayscale images in Fig. 4a and f. The thresholding technique based on fuzzy rough entropy (FRT) given in [37] and the threshold selection algorithm (OT) in [30] are considered here in order to perform segmentation. FRT algorithm detects local minima in the underlying density map and considers them as thresholds, and OT algorithm finds a predefined number of thresholds by maximizing intra-region homogeneity and inter-region heterogeneity calculated from the underlying density map.

**Observations:** Fig. 4b and c show the segmentation results obtained using the FRT algorithm on the original and the modified density maps corresponding to the image in Fig. 4a, respectively. In both the cases, three local minima are detected by FRT and they are considered as the thresholds for segmentation. As can be seen, unlike the result in Fig. 4b, the result in

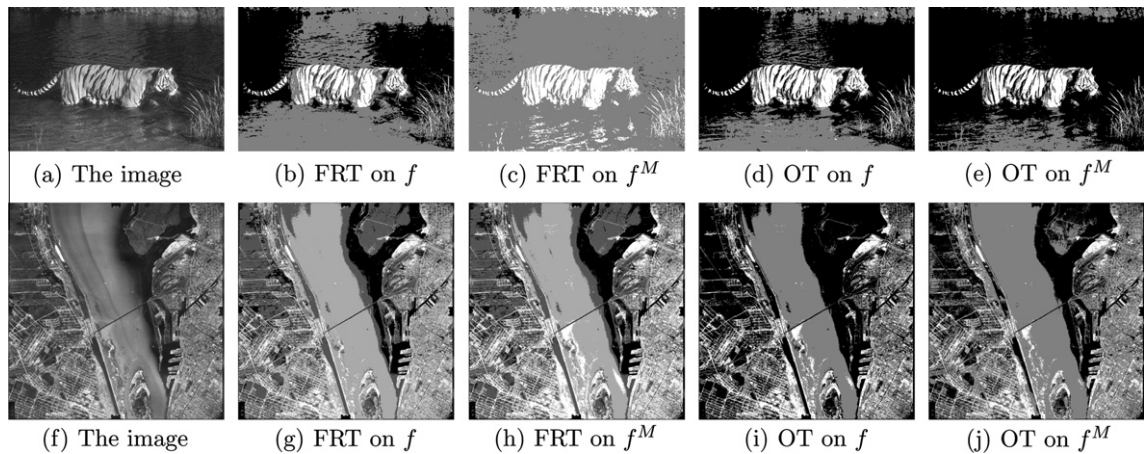


**Fig. 4.** Gray-level feature based segmentation considering original and modified density maps.

Fig. 4c puts almost the entire area with water into a single region. Fig. 4g and h show the segmentation results obtained using the FRT algorithm on the original and the modified density maps corresponding to the image in Fig. 4f, respectively. In both these cases, four local minima are detected by FRT and they are considered as the thresholds for segmentation. From Fig. 4g and h, we see no significant difference between the two results.

Fig. 4d and e show the segmentation results obtained using the OT algorithm on the original and the modified density maps corresponding to the image in Fig. 4a, respectively, and Fig. 4i and j show the same when the image in Fig. 4f is considered. The predefined number of thresholds considered by OT algorithm for segmentation is taken as 3. As can be seen, the result in Fig. 4e does marginally better than the result in Fig. 4d in assigning the entire area with water to a single region. It is evident that the segmentation result in Fig. 4j partially extracts the island from the background, unlike the result in Fig. 4i that fails completely.

**5.1.1.2. Segmentation in grayscale images based on gray-level and local homogeneity features.** Consider the segmentation of grayscale images shown in Fig. 5. The various segmentation results shown in the figure are achieved by performing clustering in two dimensional feature spaces with original ( $f$ ) or modified ( $f^M$ ) density maps corresponding to the grayscale images in Fig. 5a. The two features considered to form the two dimensional features spaces are gray level and local homogeneity. Note that, we consider the local homogeneity at a pixel in an image as the angular second moment [10] calculated by taking a neighborhood around that pixel. The clustering techniques considered here to perform segmentation are the c-means algorithm [6] and the mean shift algorithm [3,7].

**Observations:** Fig. 5b and c show the segmentation results obtained using the mean shift algorithm on the original and the modified density maps corresponding to the images in Fig. 5a, respectively. The shape of the bandwidth of the mean shift algorithm is considered as flat square and results are shown in Fig. 5b and c for different bandwidth sizes, which are mentioned in the captions. The bandwidth sizes are considered such that the results obtained using the original density map ranges from oversegmentation to undersegmentation. As can be seen, in the case of ‘Moon surface’ image, the results in Fig. 5c represent better separation of the dark and bright areas compared to the results in Fig. 5b, especially when the bandwidth size considered is  $20 \times 20$ . In the case of ‘Lena’ image, when the bandwidth size considered is  $25 \times 25$  and  $30 \times 30$ , the contents of the image are better represented by the results in Fig. 5c than the results in Fig. 5b.

Fig. 5d and e show the segmentation results obtained using the c-means algorithm on the original and the modified density maps corresponding to the images in Fig. 5a, respectively. Results are shown in Fig. 5d and e for different predefined number of clusters considered, which are mentioned in the captions. As can be seen, in the case of ‘Moon surface’ image, when the number of clusters considered is 2 and 3, the results in Fig. 5e give better representation of the different areas in the image compared to the results in Fig. 5d. However, in the case of ‘Lena’ image, the results in Fig. 5d and e are not significantly different in order to say that one is superior to the other.

**5.1.1.3. Segmentation in color images based on RGB features.** Consider the segmentation of color images shown in Fig. 6. The various segmentation results shown in the figure are achieved by performing clustering in three dimensional feature spaces with original ( $f$ ) or modified ( $f^M$ ) density maps corresponding to the color images in Fig. 6a. The three features considered to form the three dimensional features spaces are the red (R), green (G) and blue (B) components of color. Similar to the experiment represented by Fig. 5, the c-means algorithm and the mean shift algorithm are considered here for clustering.

**Observations:** Fig. 6b and c show the segmentation results obtained using the mean shift algorithm on the original and the modified density maps corresponding to the images in Fig. 6a, respectively. The shape of the bandwidth of the mean shift algorithm is considered as flat cube and results are shown in Fig. 6b and c for different bandwidth sizes, which are mentioned

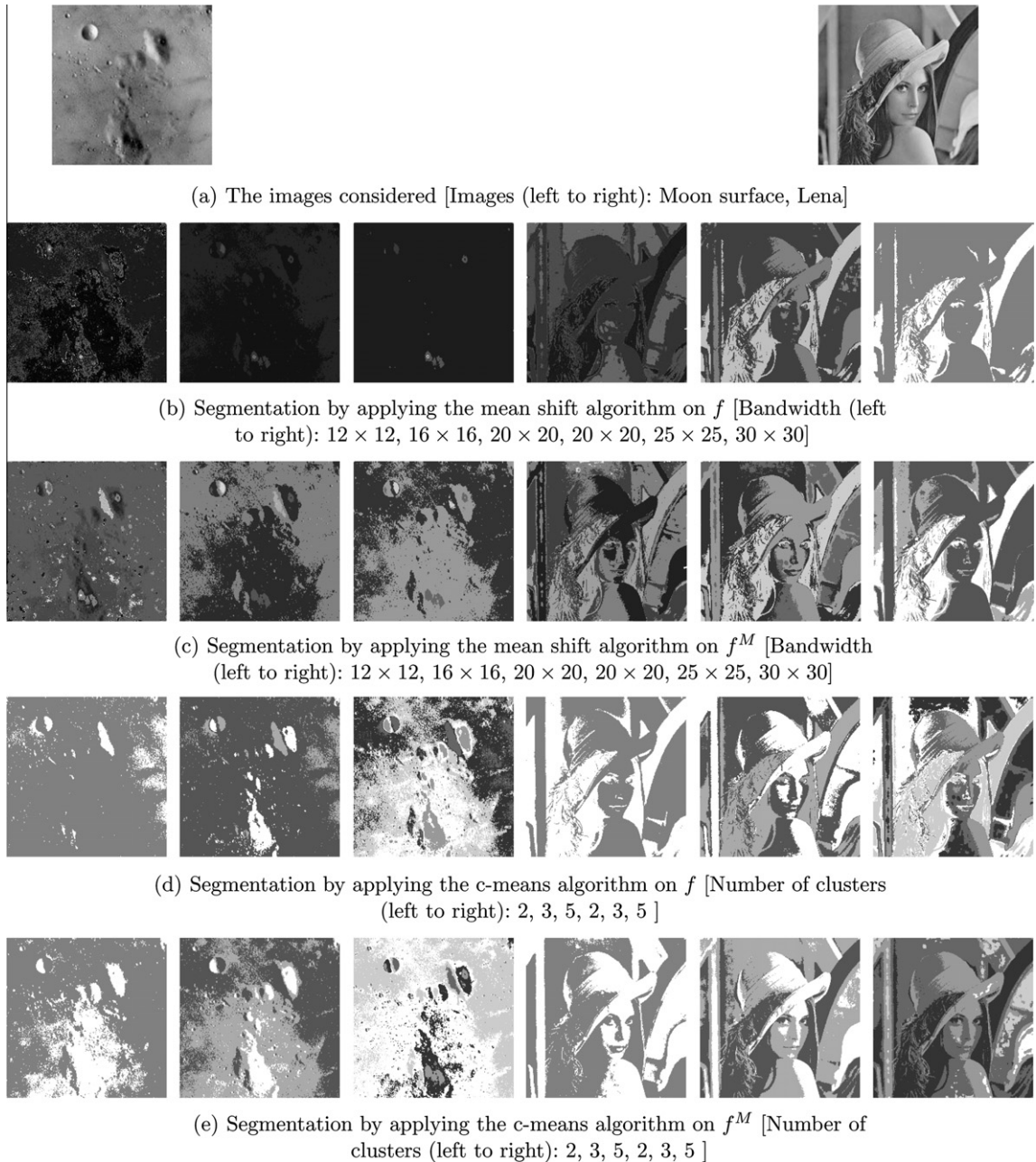


**Fig. 5.** Gray-level and local homogeneity features based segmentation considering original and modified density maps.

in the captions. The bandwidth sizes are considered such that the results obtained using the original density map ranges from oversegmentation to undersegmentation. As can be seen, in the case of ‘Pepper’ image, when the bandwidth size considered is  $25 \times 25 \times 25$  and  $30 \times 30 \times 30$ , the results in Fig. 6c put almost the entire frontal light green pepper to a single region, unlike the results in Fig. 6b. In the case of ‘Drop’ image, when the bandwidth size considered is  $60 \times 60 \times 60$ , the contents of the image are marginally better represented by the result in Fig. 6c than the result in Fig. 6b.

Fig. 6d and e show the segmentation results obtained using the c-means algorithm on the original and the modified density maps corresponding to the images in Fig. 6a, respectively. Results are shown in Fig. 6d and e for different predefined number of clusters considered, which are mentioned in the captions. As can be seen, the results in Fig. 6d and e are not significantly different, except for the case of ‘Drop’ image, when the number of clusters considered is 2. The corresponding result in Fig. 6e extracts the entire drop from the background, unlike the corresponding result in Fig. 6d that fails to do so.

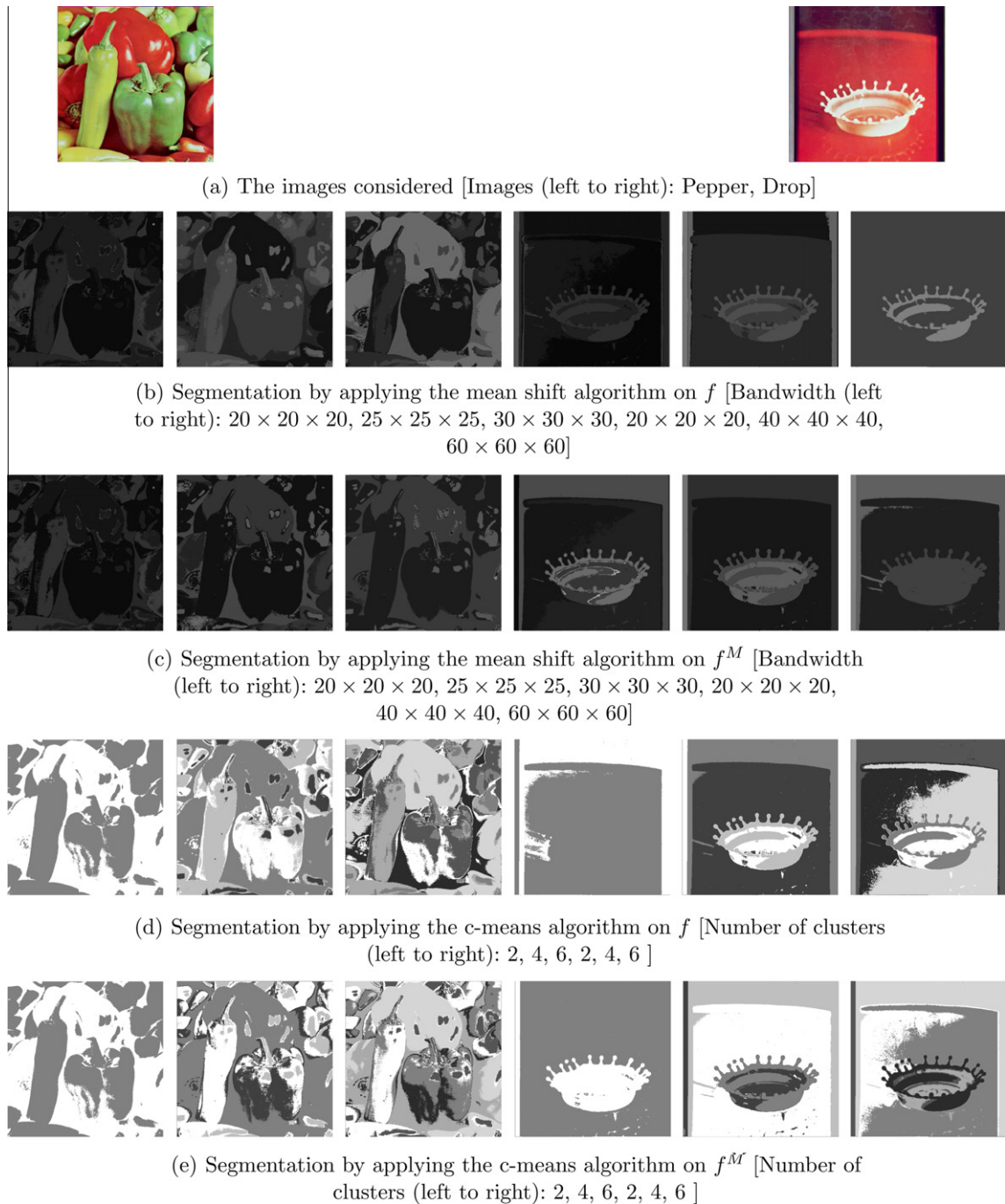


**Fig. 6.** RGB color features based segmentation considering original and modified density maps.

**5.1.1.4. Inference from the observations made in the qualitative analysis.** Let us recall that it is established in Sections 3.4.2 and 4.1.2 that the proposed density modification process enhances density map based discriminability of feature values in the underlying feature space. Such a density modification process aids feature space based segmentation and hence it can improve segmentation performance.

From the observations made in the qualitative analysis, we infer that, depending on the choice of algorithm and associated parameter values, the segmentation results obtained using modified density maps are better or as good as the segmentation results obtained using corresponding original density maps. We also infer from the observations that in the cases where the segmentation result using the original density map does not adequately represent all the contents in the image

and some objects in the image are not extracted from their backgrounds, improvement is surely achieved in segmentation performance by considering the modified density map. Note that, the aforesaid inference is the one which is exactly expected when density map based discriminability of feature values has been enhanced.

As mentioned in Section 1, it is difficult to ascertain the appropriateness of an algorithm along with associated parameter values for a feature space based segmentation task and hence the proposed density modification process finds utility in feature space based image segmentation. However, the effectiveness of the proposed density modification process can be established only when it is observed that improvement in segmentation performance using the modified density map compared to the use of original density map occurs more often than not, for a given algorithm and specific associated parameter values. Hence, we consider quantitative analysis in order to infer whether there is statistical evidence that the proposed density modification process indeed aids feature space based segmentation and improves segmentation performance.

### 5.1.2. Quantitative analysis

Here, we consider human labeled ground truth based quantitative evaluation of segmentation performance in order to carry out rigorous analysis and establish that the proposed density modification process improves feature space based image segmentation performance. Segmentation in gray scale images using gray-level and local homogeneity features is considered. The local homogeneity measure used is the angular second moment [10]. The c-means and mean shift clustering algorithms are used in two dimensional feature spaces, which are formed considering the two aforesaid features, with original and modified density maps to obtain segmentation results. The results obtained using original density maps are compared to those obtained using modified density maps in order to demonstrate the effectiveness of the proposed density modification process.

**5.1.2.1. The image dataset considered.** We consider 100 grayscale images from the ‘Berkeley Segmentation Dataset and Benchmark’ [24] (<http://www.eecs.berkeley.edu/Research/Projects/CS/vision/grouping/segbench/>). Each one of the 100 images considered are associated with multiple segmentation results hand labeled by multiple human subjects and hence we have multiple segmentation ground truths for every single image.

**5.1.2.2. The evaluation measures considered.** We use the global consistency error (GCE) and the local consistency error (LCE) measures defined in [24] in order to judge the appropriateness of segmentation results obtained by applying the c-means and mean shift clustering algorithms in image feature spaces with original and modified density maps. Consider  $S_H$  as a segmentation result hand labeled by a human subject and  $S_A$  as a segmentation result obtained applying an algorithm. The GCE and LCE measures representing the appropriateness of  $S_A$  with reference to the ground truth  $S_H$  are given as

$$GCE(S_H, S_A) = \frac{1}{n} \min \left\{ \sum_{i=1}^n E(S_H, S_A, p_i), \sum_{i=1}^n E(S_A, S_H, p_i) \right\} \quad (31)$$

$$LCE(S_H, S_A) = \frac{1}{n} \sum_{i=1}^n \min \{E(S_H, S_A, p_i), E(S_A, S_H, p_i)\} \quad (32)$$

where

$$E(S_1, S_2, p) = \frac{|R(S_1, p) \setminus R(S_2, p)|}{|R(S_1, p)|} \quad (33)$$

In the above,  $\setminus$  represents set difference,  $|x|$  represents the cardinality of a set  $x$ ,  $R(S, p)$  represents the set of pixels corresponding to the region in segmentation  $S$  that contains the pixel  $p$  and  $n$  represents the number of pixels in the image under consideration. Both GCE and LCE take values in the range  $[0, 1]$  and GCE is a tougher measure than LCE, that is,  $LCE(S_H, S_A) \leq GCE(S_H, S_A)$ . In case of both these error measures, a smaller value indicates more appropriateness of the segmentation result  $S_A$  (with reference to the ground truth  $S_H$ ). One may refer to [24] for an elaborate description of the aforesaid error measures.

**5.1.2.3. Statistical analysis of performance.** We calculate the GCE and LCE measures corresponding to all the segmentation results obtained by applying the c-means and mean shift clustering algorithms in image feature spaces having original and modified density maps, with reference to all segmentation ground truths available for every image among the 100 images considered.

When one clustering algorithm is considered for one image, a set of GCE values and a set of LCE values are obtained corresponding to both the use of original density map and the use of modified density map. Every element in a set of GCE/LCE values corresponds to one of the multiple segmentation ground truths available for the image considered and hence the number of elements in a set of GCE/LCE values obtained for an image equals the number of segmentation ground truths associated with that image.

We take the help of statistical hypothesis testing in order to compare the results obtained using the original and modified density maps, when one of the two mentioned algorithms is applied on one of the 100 images. The comparison is carried out considering the segmentation errors, that is, the sets of GCE and LCE values, obtained when the original and modified density

maps are used. We use the statistical  $t$ -test [16] assuming that the GCE values and the LCE values corresponding the use of the two density maps to be compared have come from normally distributed populations with unknown and possibly unequal variances.

We perform one-sided  $t$ -tests [16] considering the alternative hypothesis ( $H_1$ ) that 'the average segmentation error occurred while using the original density map is greater than the average segmentation error occurred while using the modified density map'. The  $p$ -value [16] obtained from such a  $t$ -test gives the probability that a superior performance obtained, when the modified density map is used, would have been due to chance alone. Such one-sided  $t$ -tests are performed for all the 100 images. The  $p$ -values obtained from these tests are shown using blue colored bars in Fig. 7.

We also perform one-sided  $t$ -tests considering the alternative hypothesis ( $H_2$ ) that 'the average segmentation error occurred while using the modified density map is greater than the average segmentation error occurred while using the original density map'. The  $p$ -value obtained from such a  $t$ -test gives the probability that a superior performance obtained, when the original density map is used, would have been due to chance alone. Such one-sided  $t$ -tests are performed for all the 100 images. The  $p$ -values obtained from these tests are shown using red colored bars in Fig. 7.

The segmentation error considered in the experiments represented by Fig. 7a and c is GCE, where Fig. 7a and c correspond to the application of c-means algorithm and mean shift algorithm, respectively. On the other hand, the segmentation error considered in the experiments represented by Fig. 7b and d is LCE, where Fig. 7b and d correspond to the application of c-means algorithm and mean shift algorithm, respectively.

Note that, we have considered two different values of parameters associated with both the clustering algorithms and hence we have two bars of the same color in each illustration given in Fig. 7. In the case of mean shift algorithm, we have considered the shape of the bandwidth as flat square and taken two different bandwidth sizes,  $20 \times 20$  and  $30 \times 30$ . In the case of c-means algorithm, we have considered two different predefined number of clusters, 5 and 10. When the aforesaid parameter values are considered, it is observed that extreme undersegmentation or oversegmentation does not occur while using the two algorithms on the original and modified density maps corresponding to each of the 100 images. This observation is important as the usage of GCE and LCE measures requires such a condition in order to appropriately calculate segmentation error value with respect to a ground truth [24].

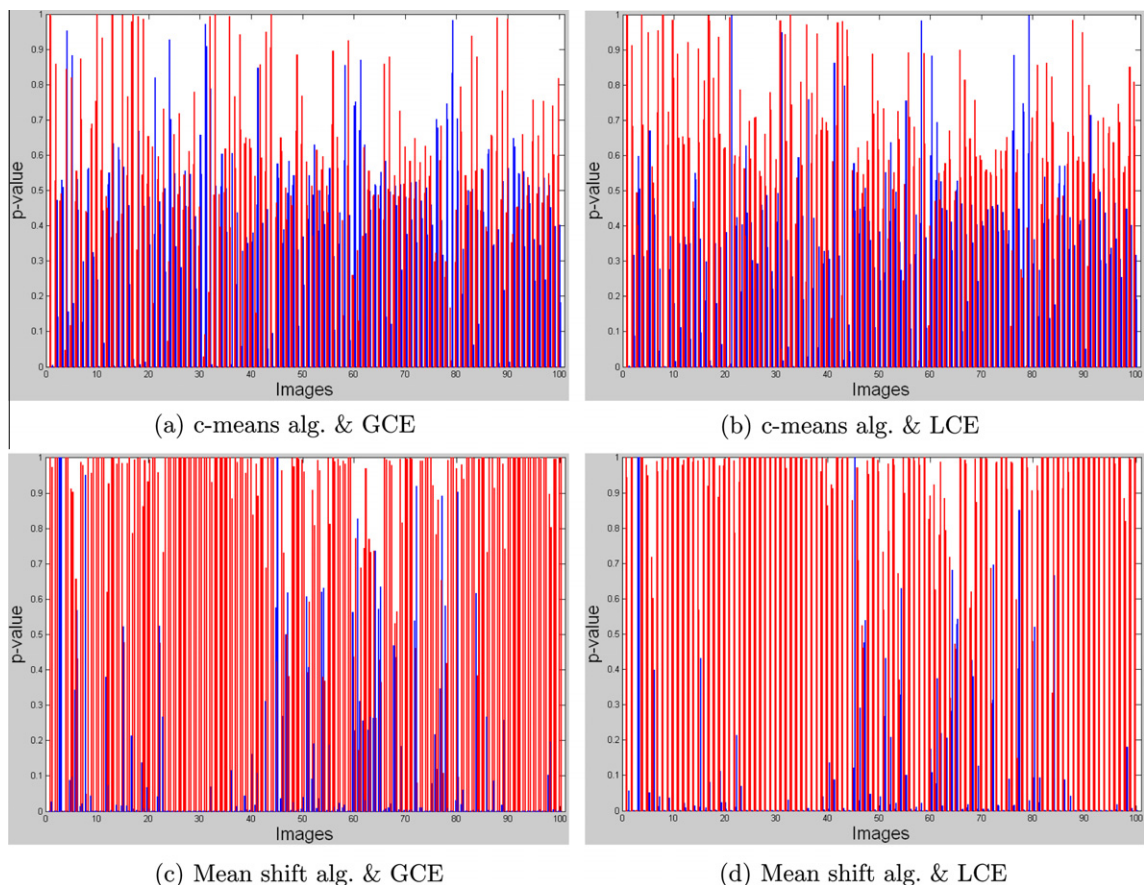


Fig. 7. The  $p$ -values obtained corresponding to the one sided  $t$ -tests with alternative hypotheses  $H_1$  and  $H_2$ .

It is evident from all the illustrations in Fig. 7 that the blue colored bars are in general shorter than the red colored bars. This signifies that, for most of the 100 images considered, it is less likely that a better segmentation performance observed when the modified density map is used is merely due to chance alone and not due to a real effect, compared to the case when the original density map is used. This observation points to the superiority of segmentation results obtained using the modified density map over those obtained using the original density map.

Now, using all the  $p$ -values (shown in Fig. 7) obtained corresponding to all the 100 images, we perform another statistical analysis in order to compare the  $p$ -values obtained performing the aforementioned  $t$ -tests with alternative hypotheses  $H_1$  and  $H_2$ . It is assumed that the  $p$ -values corresponding to the  $t$ -tests with alternative hypotheses  $H_1$  and  $H_2$  have come from normally distributed populations with unknown and possibly unequal variances. We perform two one-sided  $t$ -tests considering the following two alternative hypotheses:

$H_I$ : The average  $p$ -value obtained from the  $t$ -test with alternative hypothesis  $H_2$  is greater than the average  $p$ -value obtained from the  $t$ -test with alternative hypothesis  $H_1$ .

$H_{II}$ : The average  $p$ -value obtained from the  $t$ -test with alternative hypothesis  $H_1$  is greater than the average  $p$ -value obtained from the  $t$ -test with alternative hypothesis  $H_2$ .

The  $p$ -values obtained from the aforesaid two  $t$ -tests are given in Table 1. As can be seen from the table, we have carried out the aforesaid two  $t$ -tests considering all the  $p$ -values shown in Fig. 7, where both GCE and LCE are used, and the  $c$ -means and mean shift algorithms are employed. We observe from Table 1 that in all the cases, the  $p$ -values obtained for the  $t$ -test performed with alternative hypothesis  $H_I$  are considerably smaller than the corresponding  $p$ -values obtained for the  $t$ -test performed with alternative hypothesis  $H_{II}$ . This observation suggests that it is less likely that a smaller  $p$ -value obtained when the  $t$ -test with alternative hypothesis  $H_I$  is performed is merely due to chance alone and not due to a real effect, compared to the case when the  $t$ -test with alternative hypothesis  $H_2$  is performed. Moreover, it is interesting to note in Table 1 that most of the  $p$ -values associated with  $H_I$  is almost zero and most of the  $p$ -values associated with  $H_{II}$  is almost one. Hence, it is almost certain that a smaller  $p$ -value obtained from  $t$ -test with alternative hypothesis  $H_I$ , which points to the superiority of segmentation results obtained using the modified density map, is surely not by chance. On the other hand, it is almost certain that a smaller  $p$ -value obtained from  $t$ -test with alternative hypothesis  $H_2$ , which points to the superiority of segmentation results obtained using the original density map, is surely by chance. Therefore, from the above given analyses, we infer that there is statistical evidence that the proposed density modification process indeed aids feature space based image segmentation and improves segmentation performance.

## 5.2. Comparison of performances of the novel approach of feature space based segmentation via density modification and state-of-the-art segmentation approaches

Here, the novel approach of feature space based segmentation via density modification is compared to two popular and state-of-the-art segmentation approaches, both qualitatively and quantitatively. The two existing approaches considered are the mean-shift based approach of [4] and the graph theory based approach of [38].

It should be noted that the approaches of [4,38] form regions in an image by considering a compromising combination of gray value/color similarity and spatial proximity, whereas the proposed approach considers only similarity of feature values like gray value/color and local homogeneity, and not spatial proximity. Although the path to segmentation taken by the proposed approach is different from that taken by [4,38], a comparison between the segmentation results obtained using them would let us know the state of the proposed approach in comparison to the state-of-the-art and those which are popular.

**Table 1**

The  $p$ -values obtained corresponding to the one sided  $t$ -tests with alternative hypotheses  $H_I$  and  $H_{II}$ .

No. of clusters	Alternative hypothesis	$p$ -value	
		GCE	LCE
<i>Segmentation by c-means algorithm</i>			
5	$H_I$	$4.14 \times 10^{-13}$	$1.39 \times 10^{-12}$
	$H_{II}$	$\approx 1$	$\approx 1$
10	$H_I$	0.11938	$1.41 \times 10^{-24}$
	$H_{II}$	0.88062	$\approx 1$
<i>Bandwidth</i>			
	Alternative hypothesis	$p$ -value	
		GCE	LCE
<i>Segmentation by mean shift algorithm</i>			
Square $20 \times 20$	$H_I$	$1.54 \times 10^{-58}$	$6.4 \times 10^{-95}$
	$H_{II}$	$\approx 1$	$\approx 1$
Square $30 \times 30$	$H_I$	$1.34 \times 10^{-51}$	$4.2 \times 10^{-63}$
	$H_{II}$	$\approx 1$	$\approx 1$

### 5.2.1. Qualitative analysis

Consider the segmentation of images shown in Fig. 8. The images considered in Fig. 8a are the same that were considered in Figs. 4–6. The segmentation results shown in Fig. 8b are obtained using the proposed approach of feature space based segmentation via density modification. For each image, the best result found (from Figs. 4–6) through visual evaluation has been considered and shown in Fig. 8b. As evident from Figs. 4–6, the first two results (from left) of Fig. 8b are obtained considering gray value feature, the next two are obtained considering gray value and local homogeneity features and the last two are obtained considering color feature.

In Fig. 8c, the segmentation results shown are obtained using the approach of [4]. The publicly available EDISON segmentation system (<http://coewww.rutgers.edu/riul/research/code/EDISON>) that implements the approach is used. It requires a set of three input parameters, namely: {spatial bandwidth, color bandwidth, minimum number of pixels in a region}. The sets of parameters used to get the results are also listed (in order) in Fig. 8c. In Fig. 8d, the segmentation results shown are obtained using the approach of [38]. It requires a set of five input parameters, namely: {a parameter related to the likelihood that two pixels belong to one region in terms of color similarity, a parameter related to the likelihood that two pixels belong to one region in terms of spatial proximity, a value of Euclidean distance acting as a threshold in deciding whether two pixels are from the same region or not, a value (of normalized cut) for stopping the iterative segmentation, minimum number of pixels in a region}. The sets of parameters used to get the results are also listed (in order) in Fig. 8d. The parameters in both Fig. 8c and d are considered such that the results shown are the best ones in terms of visual evaluation.

In the segmentation of the first image (from left) in Fig. 8a, the proposed approach and the approach of [38] does better than the approach of [4] in separating the tiger out as a single object from the background. However, in the segmentation of



Fig. 8. Segmentation of grayscale and color images using various approaches.

the second image in Fig. 8a, the approach of [4] performs better in putting the entire water body into a single object in comparison to the other two. The proposed approach performs better than the other two in separating areas in terms of darkness/brightness in the segmentation of the third image in Fig. 8a. No significant difference in the performance of the three approaches can be observed from the segmentation of the fourth image in Fig. 8a. In the segmentation of the fifth image in Fig. 8a, the proposed approach performs best in extracting distinctly visible peppers as single regions, whereas the approach of [4] comes a close second. However, both of them suffer from the generation of spurious regions unlike the approach of [38]. In the segmentation of the sixth image in Fig. 8a, the proposed approach does better than the other two in separating the drop out as a single object. From the aforesaid observations, we infer that the proposed segmentation approach performs more or less as good as the approaches of [4,38].

As mentioned earlier, the proposed segmentation approach and approaches of [4,38] take different path to segmentation. The approaches of [4,38], unlike the proposed approach, consider the spatial proximity between pixels. One might encounter images where the actual semantic separation of regions are better represented in terms of only feature values and not both feature values and spatial proximity (or the other way around). Therefore, the performance of the proposed approach would be better or worse than that of [4,38] depending on the type of image encountered, which might have been the case with the results provided in Fig. 8. However, it is desirable that the segmentation performance of an algorithm, irrespective of the path it takes, is close to that of humans. Therefore, we shall now analyze the performance of the mentioned approaches in respect of the performance of humans.

### 5.2.2. Quantitative analysis

Here, we consider human labeled ground truth based quantitative evaluation of segmentation performance in order to compare the proposed approach to the existing approaches of [4,38]. Segmentation of gray scale images is considered for this purpose. The image dataset and the evaluation measures (GCE and LCE) considered are the ones that were considered in Section 5.1.2. In the case of the proposed approach, just like in Section 5.1.2, gray-level and local homogeneity features are used, and the c-means and mean shift clustering algorithms are applied in the corresponding two dimensional feature space with the modified density. In the case of both the existing approaches a particular set of required input parameters (see Section 5.2.1) is considered. For the approach of [4], the set of parameters considered is {7, 6.5, 400}, and for the approach of [38], the set of parameters considered is {5, ( $\#row \times \#column$ )/20, 2.5, 1, ( $\#row \times \#column$ )/50}. The aforesaid parameters are chosen such that extreme undersegmentation or oversegmentation does not occur for most of the images in the dataset.

We calculate the GCE and LCE measures corresponding to all the segmentation results obtained by using the proposed approach (both c-means and mean shift clustering algorithms in image feature spaces having modified density maps), the approach of [4] and the approach of [38] with reference to all segmentation ground truths available for every image among the 100 images considered. For a segmentation approach, the number of GCE/LCE values obtained corresponding to an image equals the number of segmentation ground truths available for that image.

Similar to Section 5.1.2, we consider statistical hypothesis testing in order to compare the results obtained using the mentioned existing approaches to that of the proposed approach, when one of the 100 images is considered and the proposed approach uses one of the two mentioned clustering algorithms. The comparison is carried out considering the segmentation errors, that is, the GCE and LCE values. As in Section 5.1.2, we use the statistical  $t$ -test assuming that the GCE values and the LCE values corresponding to each approach to be compared (when one image is considered) have come from normally distributed populations with unknown and possibly unequal variances.

We perform one-sided  $t$ -tests considering the alternative hypothesis ( $H_a$ ) that 'the average segmentation error occurred while using an existing approach is greater than the average segmentation error occurred while using the proposed approach'. The  $p$ -value obtained from such a  $t$ -test gives the probability that a superior performance obtained, when the proposed approach is used, would have been due to chance alone. Such one-sided  $t$ -tests are performed for all the 100 images. The  $p$ -values obtained from these tests are shown using blue colored bars in Figs. 9 and 10.

We also perform one-sided  $t$ -tests considering the alternative hypothesis ( $H_b$ ) that 'the average segmentation error occurred while using the proposed approach is greater than the average segmentation error occurred while using an existing approach'. The  $p$ -value obtained from such a  $t$ -test gives the probability that a superior performance obtained, when an existing approach is used, would have been due to chance alone. Such one-sided  $t$ -tests are performed for all the 100 images. The  $p$ -values obtained from these tests are shown using red colored bars in Figs. 9 and 10.

The  $p$ -values shown in Figs. 9 and 10 correspond to the comparison of the proposed approach to the approaches of [4,38], respectively. Each of them also correspond to two different measures of segmentation errors, namely GCE and LCE, and the use of two different clustering algorithms, namely c-means and mean shift algorithms, in the proposed approach. As in Section 5.1.2, two different values of parameters associated with both the clustering algorithms are considered. In the case of mean shift algorithm, we have considered the shape of the bandwidth as flat square and taken two different bandwidth sizes,  $20 \times 20$  and  $30 \times 30$  and in the case of c-means algorithm, we have considered two different predefined number of clusters, 5 and 10. The aforesaid considerations are appropriately mentioned in the figures.

It is evident from the illustrations in Figs. 9 and 10 which correspond to the use of c-means algorithm in the proposed approach that the red colored bars are in general shorter than the blue colored bars. However, in the illustrations that correspond to the use of mean shift algorithm in the proposed approach, except the first two (from left) in Fig. 9b, shorter blue colored bars in comparison to the red colored ones are more evident than the vice versa. In the said exceptions, equal number instances are present where blue colored bars are shorter than the red colored bars and vice versa.

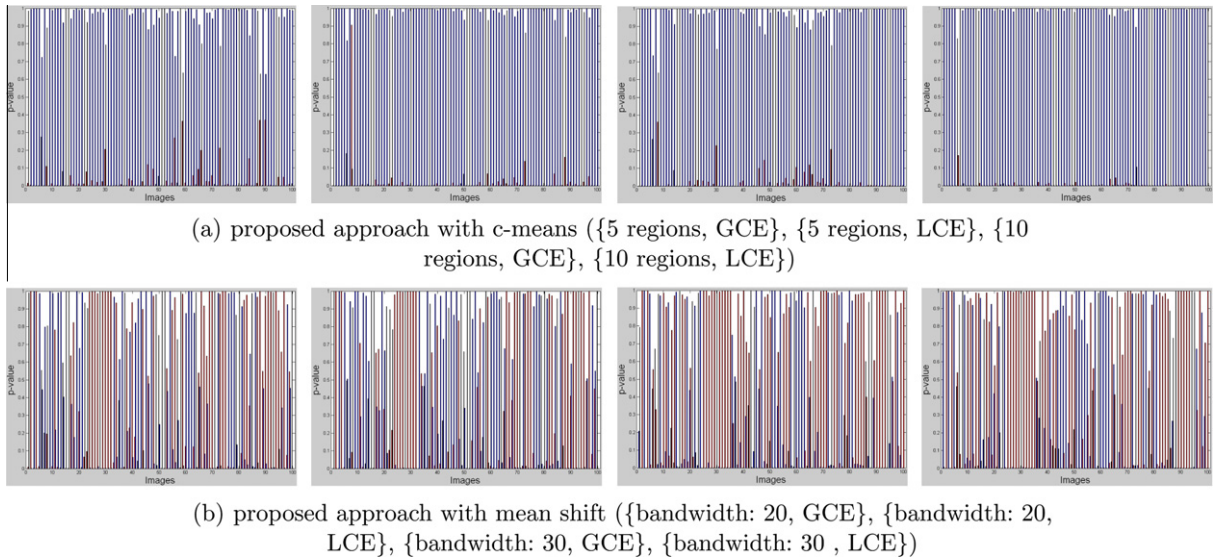


**Fig. 9.** Comparison between the proposed approach and the approach of [4]: the  $p$ -values obtained corresponding to the one sided  $t$ -tests with alternative hypotheses  $H_a$  and  $H_b$ .

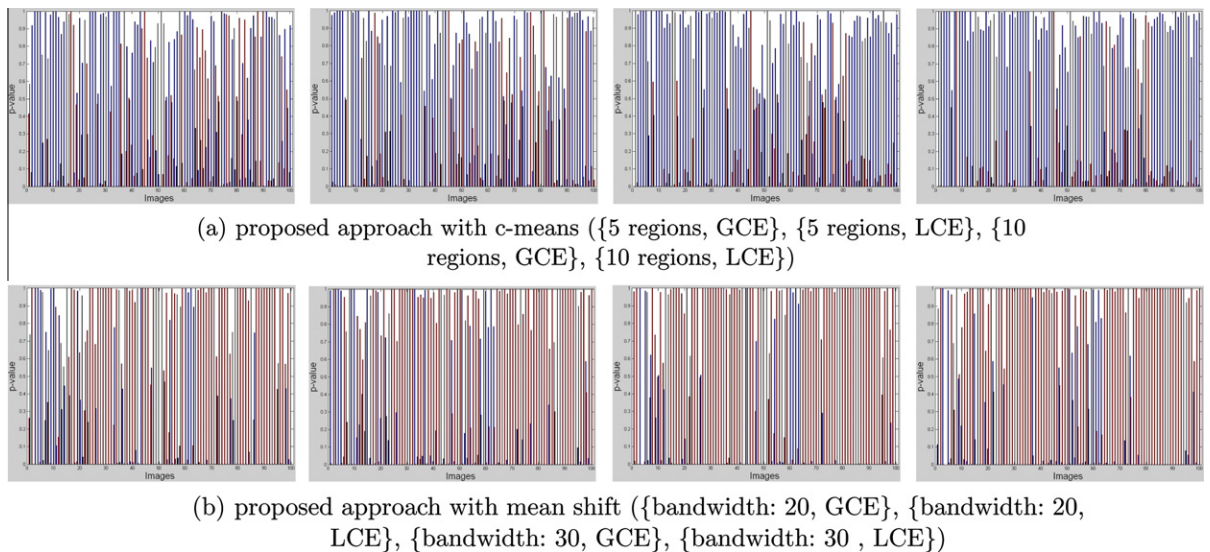


**Fig. 10.** Comparison between the proposed approach and the approach of [38]: the  $p$ -values obtained corresponding to the one sided  $t$ -tests with alternative hypotheses  $H_a$  and  $H_b$ .

The aforesaid observation signifies that, for most of the 100 images considered, it is less likely that a better segmentation performance observed when the mean shift algorithm based proposed approach is used is merely due to chance alone and not due to a real effect, compared to the case when any one of the mentioned existing approach is used. However, it is more likely that a better segmentation performance observed when the c-means algorithm based proposed approach is used is merely due to chance and not due to a real effect, compared to the case when any one of the mentioned existing approach is used. This points to the superiority of segmentation results obtained using the mean shift algorithm based proposed approach over those obtained using the approaches of [4,38], and the superiority of segmentation results obtained using the said existing approaches over those obtained using c-means algorithm based proposed approach.

We now perform statistical analysis (one-sided  $t$ -tests) in order to compare the  $p$ -values obtained performing the aforementioned  $t$ -tests with alternative hypotheses  $H_a$  and  $H_b$ . It is assumed that the  $p$ -values corresponding to the  $t$ -tests with alternative hypotheses  $H_a$  and  $H_b$  have come from normally distributed populations with unknown and possibly unequal variances.

**Table 2**

Comparison between the proposed approach and the approach of [4]: the  $p$ -values obtained corresponding to the one sided  $t$ -tests with alternative hypotheses  $H_A$  and  $H_B$ .

No. of clusters	Alternative hypothesis	$p$ -value	
		GCE	LCE
<i>Comparison of segmentation by using <math>c</math>-means algorithm on <math>f^M</math> with that of the algorithm in MS</i>			
5	$H_A$	$\approx 1$	$\approx 1$
	$H_B$	$4.6250 \times 10^{-154}$	$5.2866 \times 10^{-144}$
10	$H_A$	$\approx 1$	$\approx 1$
	$H_B$	$7.7295 \times 10^{-185}$	$8.3212 \times 10^{-275}$
Bandwidth	Alternative hypothesis	$p$ -value	
		GCE	LCE
<i>Comparison of segmentation by using mean shift algorithm on <math>f^M</math> with that of the algorithm in MS</i>			
Square $20 \times 20$	$H_A$	0.1409	0.6205
	$H_B$	0.8591	0.3795
Square $30 \times 30$	$H_A$	$5.5882 \times 10^{-8}$	$9.3703 \times 10^{-6}$
	$H_B$	$\approx 1$	$\approx 1$

**Table 3**

Comparison between the proposed approach and the approach of [38]: the  $p$ -values obtained corresponding to the one sided  $t$ -tests with alternative hypotheses  $H_A$  and  $H_B$ .

No. of clusters	Alternative hypothesis	$p$ -value	
		GCE	LCE
<i>Comparison of segmentation by using <math>c</math>-means algorithm on <math>f^M</math> with that of the algorithm in MS</i>			
5	$H_A$	$\approx 1$	$\approx 1$
	$H_B$	$4.8301 \times 10^{-11}$	$7.7161 \times 10^{-15}$
10	$H_A$	$\approx 1$	$\approx 1$
	$H_B$	$8.5422 \times 10^{-38}$	$8.2424 \times 10^{-37}$
Bandwidth	Alternative hypothesis	$p$ -value	
		GCE	LCE
<i>Comparison of segmentation by using mean shift algorithm on <math>f^M</math> with that of the algorithm in NC</i>			
Square $20 \times 20$	$H_A$	$8.3267 \times 10^{-16}$	0
	$H_B$	$\approx 1$	1
Square $30 \times 30$	$H_A$	$3.1945 \times 10^{-33}$	$1.5093 \times 10^{-36}$
	$H_B$	$\approx 1$	$\approx 1$

We perform two one-sided  $t$ -tests considering the following two alternative hypotheses:

$H_A$ : The average  $p$ -value obtained from the  $t$ -test with alternative hypothesis  $H_b$  is greater than the average  $p$ -value obtained from the  $t$ -test with alternative hypothesis  $H_a$ .

$H_B$ : The average  $p$ -value obtained from the  $t$ -test with alternative hypothesis  $H_a$  is greater than the average  $p$ -value obtained from the  $t$ -test with alternative hypothesis  $H_b$ .

Table 2 corresponds to the  $t$ -tests performed considering all the  $p$ -values shown in Fig. 9 corresponding to all the 100 images in order to compare the proposed approach to the approach of [4]. Table 3 corresponds to the  $t$ -tests performed considering all the  $p$ -values shown in Fig. 10 corresponding to all the 100 images in order to compare the proposed approach to the approach of [38]. We observe the following from the Tables 2 and 3:

- (1) The  $p$ -values obtained for the  $t$ -test performed with alternative hypothesis  $H_A$  are considerably smaller than the corresponding  $p$ -values obtained for the  $t$ -test performed with alternative hypothesis  $H_B$  when mean-shift algorithm based proposed approach is considered, except the case of LCE and bandwidth  $20 \times 20$ .

- (2) The  $p$ -values obtained for the  $t$ -test performed with alternative hypothesis  $H_B$  are considerably smaller than the corresponding  $p$ -values obtained for the  $t$ -test performed with alternative hypothesis  $H_A$  when c-means algorithm based proposed approach is considered

The first observation suggests that it is almost unlikely that a smaller  $p$ -value obtained when the  $t$ -test with alternative hypothesis  $H_a$  is performed is merely due to chance alone and not due to a real effect compared to the case when the  $t$ -test with alternative hypothesis  $H_b$  is performed, when the proposed approach is based on mean-shift algorithm. However, on the contrary, the second observation suggests that when the proposed approach is based on c-means algorithm, the aforesaid phenomenon is very likely. This points to the superiority of performance of the mean shift algorithm based proposed approach over the approaches of [4,38], and to the inferiority of performance of c-means algorithm based proposed approach compared to that of the said existing approaches. Therefore, there is statistical evidence that the proposed approach is the best of the lot considered in this section, provided that it uses the mean shift clustering algorithm.

## 6. Conclusion

A density modification framework that enhances density map based discriminability of feature values in a feature space has been proposed in this paper in order to aid feature space based segmentation in images. In the framework, fuzzy set theory has been used to associate a position-dependent property with each sample in a feature space of an image. The associated property has then been embedded into the density map of the samples in the feature space resulting in its modification. The use of beam theory from the field of solid mechanics has been proposed in order to carry out the property association and embedding. The appropriateness of the aforesaid usage has also been established.

Qualitative and quantitative experimental results of segmentation in images have been given, and comparisons have been made between the results obtained with and without performing density modification in order to demonstrate the utility and effectiveness of the proposed density modification framework. It has been shown the proposed density modification process indeed aids segmentation tasks, and improves their performance. The usefulness the novel approach of feature space based segmentation via density modification has been demonstrated through comparisons with state-of-the-art segmentation approaches.

As a natural follow-up of the work in this paper, comparisons with other methods that improve performance of feature space based segmentation systems may be performed. Note that most of such methods are specific to particular systems and employ different approaches to achieve the improvement. Such comparisons may result in a good investigation that would analyze the effectiveness of the proposed framework inspite of its general nature, that is, its applicability with any feature space based segmentation system. It should also be noted that some of the existing methods for improving performance of feature space based segmentation could also be used in combination with the proposed framework.

## Acknowledgements

The authors thank the anonymous referees for their valuable suggestions. S.K. Pal would like to thank the Government of India for the J.C. Bose National Fellowship.

## References

- [1] Z.A. Aghbari, R.A. Haj, Hill-manipulation: an effective algorithm for color image segmentation, *Image and Vision Computing* 24 (8) (2006) 894–903.
- [2] A. Broder, A. Rosenfeld, Gradient magnitude as an aid in color pixel classification, *IEEE Transactions on Systems, Man, and Cybernetics – Part B* 11 (3) (1981) 248–249.
- [3] Y. Cheng, Mean shift, mode seeking, and clustering, *IEEE Transactions on Pattern Analysis and Machine Intelligence* 17 (8) (1995) 790–799.
- [4] D. Comaniciu, P. Meer, Mean shift: a robust approach toward feature space analysis, *IEEE Transactions on Pattern Analysis and Machine Intelligence* 24 (5) (2002) 603–619.
- [5] S. Das, S. Sil, Kernel-induced fuzzy clustering of image pixels with an improved differential evolution algorithm, *Information Sciences* 180 (8) (2010) 1237–1256.
- [6] R.O. Duda, P.E. Hart, D.G. Stock, *Pattern Classification*, second ed., Wiley Interscience, USA, 2000.
- [7] K. Fukunaga, L.D. Hostetler, The estimation of the gradient of a density function, with applications in pattern recognition, *IEEE Transactions on Information Theory* 21 (1) (1975) 32–40.
- [8] M. Grundland, N.A. Dodgson, Automatic contrast enhancement by histogram warping, in: *Proceedings of International Conference on Computer Vision and Graphics, Computational Imaging and Vision*, vol. 32, 2004.
- [9] L. Gupta, T. Sortrakul, A gaussian mixture-based image segmentation algorithm, *Pattern Recognition* 31 (3) (1998) 315–325.
- [10] R.M. Haralick, K. Shanmugam, I. Dinstein, Textural features for image classification, *IEEE Transactions on Systems, Man, and Cybernetics* 3 (6) (1973) 610–621.
- [11] A.K. Jain, M.N. Murthy, P.J. Flynn, Data clustering: a review, *ACM Computing Surveys* 31 (3) (1999) 264–323.
- [12] J.N. Kapur, P.K. Sahoo, A.K.C. Wong, A new method for gray-level picture thresholding using the entropy of the histogram, *Computer Vision, Graphics, and Image Processing* 29 (1985) 273–285.
- [13] G. Klir, B. Yuan, *Fuzzy Sets and Fuzzy Logic: Theory and Applications*, Prentice Hall, New Delhi, India, 2005.
- [14] C.H. Lee, O.R. Zaiane, H.H. Park, J. Huang, R. Greiner, Clustering high dimensional data: a graph-based relaxed optimization approach, *Information Sciences* 178 (23) (2008) 4501–4511.
- [15] J.S. Lee, S. Olafsson, Data clustering by minimizing disconnectivity, *Information Sciences* 181 (4) (2011) 732–746.
- [16] E.L. Lehmann, J.P. Romano, *Testing Statistical Hypothesis*, third ed., Springer, USA, 2005.
- [17] C. Li, R. Huang, Z. Ding, J.C. Gatenby, D.N. Metaxas, J.C. Gore, A level set method for image segmentation in the presence of intensity inhomogeneities with application to MRI, *IEEE Transactions on Image Processing* 20 (7) (2011) 2007–2016.

- [18] Q. Li, N. Mitianoudis, T. Stathaki, Spatial kernel k-harmonic means clustering for multi-spectral image segmentation, *IET Image Processing* 1 (2) (2007) 156–167.
- [19] X. Li, H.S. Wong, S. Wu, A fuzzy minimax clustering model and its applications, *Information Sciences* 186 (1) (2012) 114–125.
- [20] Y.W. Lim, S.U. Lee, On the color image segmentation algorithm based on the thresholding and the fuzzy c-means techniques, *Pattern Recognition* 23 (9) (1990) 935–952.
- [21] P. Maji, M.K. Kundu, B. Chanda, Second order fuzzy measure and weighted co-occurrence matrix for segmentation of brain MR images, *Fundamenta Informaticae* 88 (1–2) (2008) 161–176.
- [22] P. Maji, S.K. Pal, Rough set based generalized fuzzy c-means algorithm and quantitative indices, *IEEE Transactions on Systems, Man, and Cybernetics – Part B* 37 (6) (2007) 1529–1540.
- [23] D. Malyszko, J. Stepaniuk, Adaptive multilevel rough entropy evolutionary thresholding, *Information Sciences* 180 (7) (2010) 1138–1158.
- [24] D. Martin, C. Fowlkes, D. Tal, J. Malik, A database of human segmented natural images and its application to evaluating segmentation algorithms and measuring ecological statistics, in: *Proceedings of 8th International Conference on Computer Vision*, vol. 2, 2001.
- [25] F. Melgani, Robust image binarization with ensembles of thresholding algorithms, *Journal of Electronic Imaging* 15 (2) (2006) 023010.
- [26] F. Meyer, Levelings, image simplification filters for segmentation, *Journal of Mathematical Imaging and Vision* 20 (1–2) (2004) 59–72.
- [27] S. Mitra, P.P. Kundu, Satellite image segmentation with shadowed c-means, *Information Sciences* 181 (17) (2011) 3601–3613.
- [28] C.A. Murthy, S.K. Pal, Histogram thresholding by minimizing graylevel fuzziness, *Information Sciences* 60 (1–2) (1992) 107–135.
- [29] A.H. Nayfeh, P.F. Pai, *Linear and Nonlinear Structural Mechanics*, Wiley Series in Nonlinear Science, John Wiley & Sons, New York, USA, 2004.
- [30] N. Otsu, A threshold selection method from gray-level histogram, *IEEE Transactions on Systems, Man, and Cybernetics* 9 (1) (1979) 62–66.
- [31] P.Y. Pai, C.C. Chang, Y.K. Chan, M.H. Tsai, An adaptable threshold detector, *Information Sciences* 181 (8) (2011) 1463–1483.
- [32] S.K. Pal, A. Ghosh, Image segmentation using fuzzy correlation, *Information Sciences* 62 (3) (1992) 223–250.
- [33] S.K. Pal, R.A. King, A.A. Hashim, Automatic grey level thresholding through index of fuzziness and entropy, *Pattern Recognition Letters* 1 (3) (1983) 141–146.
- [34] I.B. Prasad, *Applied Mechanics and Strength of Materials*, fifth ed., Khanna Publishers, Delhi, India, 1983.
- [35] A. Rosenfeld, L.S. Davis, Image segmentation and image models, *Proceedings of the IEEE* 67 (5) (1979) 764–772.
- [36] B. Schölkopf, A. Smola, K.R. Müller, Nonlinear component analysis as a kernel eigenvalue problem, *Neural Computation* 10 (5) (1998) 1299–1319.
- [37] D. Sen, S.K. Pal, Generalized rough sets, entropy, and image ambiguity measures, *IEEE Transactions on Systems, Man, and Cybernetics – Part B* 39 (1) (2009) 117–128.
- [38] J. Shi, J. Malik, Normalized cuts and image segmentation, *IEEE Transactions on Pattern Analysis and Machine Intelligence* 22 (8) (2000) 888–905.
- [39] B.W. Silverman, *Density Estimation for Statistics and Data Analysis*, Chapman & Hall/CRC Press, New York, USA, 1986.
- [40] A. Sofou, P. Maragos, Generalized flooding and multicue PDE-based image segmentation, *IEEE Transactions on Image Processing* 17 (3) (2008) 364–376.
- [41] L. Wang, H. Ji, X. Gao, Image segmentation by a robust clustering algorithm using Gaussian estimator, in: *Proceedings of International Conference on Image Analysis and Recognition*, Lecture Notes in Computer Science, vol. 3211, 2004.
- [42] Y. Wang, J. Ostermann, Y.Q. Zhang, *Video Processing and Communications*, Signal Processing Series, Prentice Hall, USA, 2002.
- [43] J.S. Wezka, A. Rosenfeld, Histogram modification for threshold selection, *IEEE Transactions on Systems, Man, and Cybernetics* 9 (1) (1979) 38–52.
- [44] D. Yang, L. Jiao, M. Gong, F. Liu, Artificial immune multi-objective SAR image segmentation with fused complementary features, *Information Sciences* 181 (13) (2011) 2797–2812.
- [45] Z. Yang, F.L. Chung, W. Shitong, Robust fuzzy clustering-based image segmentation, *Applied Soft Computing* 9 (1) (2009) 80–84.
- [46] K. Zhang, J.T. Kwok, Simplifying mixture models through function approximation, *IEEE Transactions on Neural Networks* 21 (4) (2010) 644–658.
- [47] L. Zhang, Q. Cao, A novel ant-based clustering algorithm using the kernel method, *Information Sciences* 181 (20) (2011) 4658–4672.
- [48] L. Zhang, Q. Ji, A Bayesian network model for automatic and interactive image segmentation, *IEEE Transactions on Image Processing* 20 (9) (2011) 2582–2593.